Telecommun Syst (2015) 59:93–110
DOI 10.1007/s11235-014-9886-3

An energy efficient DOA estimation algorithm for uncorrelated and coherent signals in virtual MIMO systems

Liangtian Wan · Guangjie Han · Joel J. P. C. Rodrigues · Weijian Si · Naixing Feng

Published online: 19 November 2014

Abstract The multiple input and multiple output (MIMO) and smart antenna (SA) technique have been widely accepted as promising schemes to improve the spectrum efficiency and coverage of mobile communication systems. The definition of direction-of-arrival (DOA) estimation is that multiple directions of incident signals can be estimated simultaneously by some algorithms using the received data. The conventional DOA estimation of user equipments (UEs) is one by one, which is named as sequential scheme. The Virtual MIMO (VMIMO) scheme is that the base station (BS) estimates the DOAs of UEs in a parallel way, which adopts the SA simultaneously. Obviously, when the power is fixed, the VMIMO scheme is much more energy efficient than the sequential scheme. In VMIMO scheme, a set of UEs are grouped together to simultaneously communicate with the BS on a given resource block. Then the BS using multiple antennas can estimate the 2D-DOA of the UEs in the group simultaneously. Based on VMIMO system, the 2D-DOA estimation algorithm for uncorrelated and coherent signals is proposed in this paper. The special structure of mutual coupling matrix (MCM) of uniform linear array (ULA) is applied to eliminate the effect of mutual coupling. The 2D-DOA of uncorrelated signals can be estimated by DOA-matrix method. The parameter pairing between azimuth and elevation is accomplished. Then these estimations are utilized to get the mutual coupling coefficients. Based on spatial smoothing and DOA matrix method, the 2D-DOA of coherent signals can be estimated. The Cramer–Rao lower bound is derived at last. Simulation results demonstrate the effectiveness and performance of the proposed algorithm.

Keywords VMIMO system · DOA estimation · Multipath · Mutual coupling

L. Wan · W. Si (✉)
Department of Information and Communication Engineering, Harbin Engineering University, Harbin 150001, China
e-mail: swj0418@263.net

L. Wan
e-mail: wanliangtian1@163.com

G. Han (✉)
Department of Information and Communication Systems, Hohai University, Changzhou 213022, China
e-mail: hanguangjie@gmail.com

J. J. P. C. Rodrigues
Instituto de Telecomunicações, University of Beira Interior, 6201-001 Covilhã, Portugal

J. J. P. C. Rodrigues
University of ITMO, St. Petersburg 197101, Russia
e-mail: joeljr@ieee.org

N. Feng
Institute of Electromagnetics and Acoustics, Xiamen University, Xiamen 361005, China
e-mail: fengnaixing@gmail.com

1 Introduction

The demands for higher data rates over longer distances, scarcity of mobile wireless resources, and need for efficiency of spectrum usage [17,43–45] have motivated the development of multiple input and multiple output (MIMO) antenna over orthogonal frequency division multiplexing (OFDM) communication systems [1,7,29,32]. MIMO becomes increasingly essential as the demand for broadband wireless data transmitter increases. MIMO antenna implementation requires multiple antennas and multiple-RF chains in both the receivers and senders sides. However, because the size of User Equipments (UEs) is very small, the conventional MIMO antenna technologies become challenging, especially

when it comes to placing multiple-RF chains in these devices, which are usually bulky [23]. Due to this, technologies such as transmit antenna selection [6] and Spatial Modulation [24] have been proposed that exploit the presence of multiple antennas with a single-RF chain. The energy consumption of single-RF chain is much less than that of multiple-RF chains. The Massive MIMO, also known as "large-scale antenna systems" , contains extreme base station and device densities and unprecedented numbers of antennas in fifth generation (5G) system. The energy efficiency problem is the first thing to deal with. As specified in our stated requirements for 5G, the energy efficiency of the communication chain typically measured in either Joules/bit or bits/Joule will need to improve by about the same amount as the data rate just to maintain the power consumption. And by more if such consumption is to be reduces. This implies a several-order-of-magnitude increase in energy efficiency, which is extremely challenging.

An alternative approach is that a set of UEs with single antenna can be grouped together and communicate with the Base Station (BS) simultaneously on the same resource block. The BS equipped with a set of UEs constructs a Virtual MIMO (VMIMO) system. In the VMIMO system, antennas at the terminals are virtually jointed together to form a so-called virtual antenna array. The vast proliferation of the mobile devices along with the increasing data demands pave the way for the 5G wireless communication systems. The VMIMO is believed to be a key technology for 5G mobile communications techniques. It enables one to make use of all the neighboring terminals and amortize the cost of multiple antennas; hence, a large MIMO channel can be created to increase capacity significantly as well as improve error rate performance. The use of smart antenna technique is promising to reduce interference, increase coverage and provide geographic information. There are two basic types of smart antennas. One is the fixed multi-beam antenna. While UE is moving, different beams are turned on or off. The other type is the adaptive array of antennas. In both types of smart antenna, the Direction-of-Arrival (DOA) estimation [14,16] for UEs is crucial.

Multiple Signal Classification (MUSIC) [27,28] and Estimation of Signal Parameters via Rotational Invariance Technique (ESPRIT) [26] have been widely implemented in real-time processing [18] for DOA estimation. It is due to that the computational complexity is not high and the resolution of them is acceptable. However, when multipath propagation caused by reflection and refraction exists, the incident signals may be coherent, thus the conventional DOA estimation algorithms can not be used. In order to deal with the coherent signals, the spatial smoothing technique can be used as a pre-processing step [33]. The matrix reconstruction [10,11] and eigenvector singular value decomposition [3,4] are alternative effective approaches based on the spatial smoothing techniques.

At present, the DOA estimation of mixed signals (uncorrelated and coherent signals) has received considerable attention. Some new differencing methods were proposed to estimate the DOA of uncorrelated and coherent signals separately [21,25,40]. In these methods, the DOA of uncorrelated signals has been estimated at first, and then the contribution of the uncorrelated signals has been eliminated for estimating the DOA of coherent signals. However, in some cases, the resulting matrix which is corresponding to the coherent signals may be canceled completely to be zero [20]. Based on ESPRIT and the oblique projection technique, the DOA and mutual coupling coefficients are estimated [37]. In real application, the 2D-DOA estimation (i.e., elevation and azimuth) of multiple signals is also an important parameter. Based on the differencing method, the Z-shaped or uniform rectangular planar [41,42] were used for estimating 2D-DOA. However, these methods have the same problem as [21,25,40]. The DOAs of uncorrelated signals are first estimated by a modified 2D ESPRIT. Then the contributions of uncorrelated signals and noises are eliminated after performing a subtraction operation on the elements of the covariance matrix and only those of coherent signals remain [35]. Based on propagator method, the 2D-DOA estimation of a mixed signal impinging on a simple structured planar array which consists of two parallel uniform linear arrays (ULAs) was proposed. However, the computational complexity of the algorithm is tremendous because of the spectrum speak searching [30]. In addition, the effect of mutual coupling of the 2D-DOA estimation algorithms mentioned above has not been taken into consideration. Based on the matrix transformation, the mutual coupling coefficients are estimated to calibrate the effect of mutual coupling [12]. Based on the generalized eigenvalues utilizing signal subspace eigenvectors (GEESE) algorithm for uniform linear array (ULA), the DOA can be accurately estimated without any calibration sources and the mutual coupling coefficients is also proposed [38].

The conventional DOA estimation of UEs is one by one, which is named as sequential scheme. The VMIMO scheme is that the BS estimates the DOA in a parallel way, which adopts the SA simultaneously. Obviously, when the power is fixed, the VMIMO scheme is much more energy efficient than the sequential scheme. The details of energy efficient analysis is shown in Sect. 2. However, when the UEs communicate with the BS, the signal may suffer from the multipath propagation due to the various reflections. It is caused by reflectors and scatters during the course of signal propagation. The buildings and hills are the main reflectors which cause the multipath propagation. The received signals of the BS would be highly correlated or even coherent. Thus the coherency among the signals is a critical problem that the VMIMO scheme needs to deal with. The DOA estimation algorithm design is a great challenge for the VMIMO scheme when the DOA estimation is accomplished. In real applica-

tions, the DOA estimation of UEs contains two dimensional, i.e., azimuth angle and elevation angle. The 2D-DOA estimation is more meaningful. Moreover, the mutual coupling among the elements would inevitably affect the DOA estimation performance. In order to obtain a high resolution of the DOA estimation, the mutual coupling effect has to be eliminated or compensated. Thus the 2D-DOA estimation problem in the VMIMO scheme including multipath propagation and mutual coupling has to be solved.

This paper focuses on the 2D-DOA estimation of uncorrelated and coherent signals in the presence of unknown mutual coupling in VMIMO systems. The special structure of mutual coupling matrix (MCM) of ULA is applied to eliminate the effect of mutual coupling. The 2D-DOA of uncorrelated signals can be estimated by DOA-matrix method. The parameter pairing of uncorrelated signals between azimuth and elevation is accomplished. Then these estimations are utilized to get the mutual coupling coefficients. The oblique operator is used to eliminate the information of the uncorrelated signals. Based on spatial smoothing and DOA matrix method, the 2D-DOA of coherent signals can be estimated. Compared with the FBSS-based method, the proposed algorithm can estimate more signals. The computational complexity of the proposed algorithm is lower than that of the FBSS-based method. The uncorrelated and coherent signals of the proposed algorithm can be carried out in parallel because there is no inherent relationship between them. The processing can be further speeded up in practical application. However, the DOA estimation of Automatic Weighted Subspace Fitting (AWSF) algorithm [5] need multi-dimensional nonlinear optimization searching, and large numbers of UEs in the VMIMO system lead to large computational cost.

The paper is organized as follows. The energy efficient analysis is given in Sect. 2. The VMIMO system model and narrowband signal model are introduced in Sect. 3. The DOA estimation of uncorrelated signals is then considered in detail in Sect. 4. In Sect. 5, the mutual coupling coefficients estimation is elaborated. The DOA estimation of coherent signals is given in Sect. 6. The algorithm steps and some concluding remarks for this method are given in Sect. 7. In Sect. 8, simulation results are shown and discussed to validate the effectiveness of our method. The derivation of Cramer–Rao bound (CRB) is given in the appendix.

2 The energy efficient analysis

Consider a system that a BS communicates with M UEs. The smart antenna technique is used in the BS and only one antenna is installed in the UEs. Therefore, the DOA estimation is an important problem to solve in the system. Generally, there are two methods to estimate the DOA. The first scheme is to estimate the DOAs of UEs one by one, which is named as sequential scheme. The second scheme is that the BS estimates the DOA in a parallel way, which is named as the VMIMO scheme. For each time, the number of the incident signals coming from the UEs is one, then the sequential scheme can exploit most DOA estimation algorithms to achieve high estimation accuracy and resolution. It can be seen obviously that the VMIMO scheme is much more efficient than the sequential scheme. In order to have an intuitionistic interpretation, an example is given as follows. A snapshot time T_{sp} is taken to estimate the DOA of one UE. For M UEs, $M \times T_{sp}$ time for snapshots has to be taken for the sequential scheme and M times DOA estimation have to be done. The sequential scheme is suitable for the condition that the processing capacity of the BS is weak. If the BS has a strong processing capacity, the VMIMO scheme should be adopted. We assume that the VMIMO scheme can estimate K_V DOAs . i.e., the DOAs of K_V UEs are estimated simultaneously. Then $\left\lceil \frac{M}{K_V} \right\rceil$ times DOA estimation have to be taken for the BS and the snapshot time is reduced to $\left\lceil \frac{M}{K_V} \right\rceil \times T_{sp}$. The power of BS is assumed to be P_t, the energy consumption of sequential scheme is $P_t \times M T_{sp}$. The VMIMO scheme is $P_t \left\lceil \frac{M}{K_V} \right\rceil T_{sp}$, which takes less energy consumption than that of sequential scheme. More details can be found in [5]. Based on the energy efficient analysis, the VMIMO scheme is adopted. Then the DOA estimation algorithm based on the VMIMO scheme is proposed in the following.

3 The system model and problem formulation

In this section, the VMIMO system is constructed at first. Next, the mathematical model of 2D-DOA estimation for uncorrelated and coherent signals is given, and the array is two parallel ULAs.

3.1 The VMIMO system model

As shown in Fig. 2, the smart antenna technique is employed in BS for DOA estimation. The BS communicates with M UEs. Based on the smart antenna technique, the DOA estimation of UEs becomes more easily. Because of the signal reflection caused by the building, the multipath propagation is taken into consideration. There are two feasible schemes to estimate DOA. One is called the sequential scheme that the BS estimates the DOA of the UEs one by one sequentially. It is commonly used in the traditional communication framework. Another is called the VMIMO scheme that a set of UEs with single antenna can be grouped together to communicate with the BS with multiple antennas on the same

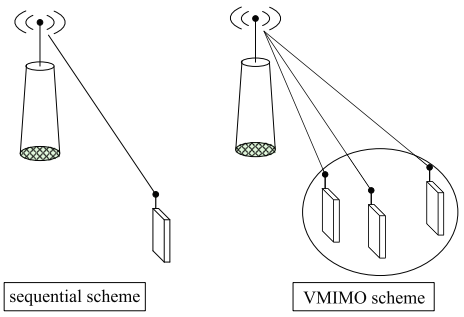

Fig. 1 The sequential scheme and VMIMO scheme

resource block. Then a Virtual MIMO system is structured [17]. These two schemes are shown in Fig. 1.

3.2 The Problem Formulation of DOA Estimation

Consider K narrowband far-field signals impinging on a planar array consisting of two parallel ULAs. Assume that the smart antenna of the BS is the array antenna with two parallel ULAs. The configuration of the two parallel ULAs is shown in Fig. 3.

Each ULA has N identical elements with inter element spacing d_y, and the spacing between two ULAs is d_x. The sub-array 1 and sub-array 2 consist of elements $y_1 \sim y_N$ and elements $x_1 \sim x_N$, respectively. The incident signals are a mixture of coherent and uncorrelated signals with distinct 2D-DOAs (α_k, β_k). Assume that there are K_c coherent signals undergoing multipath propagation and K_u uncorrelated signals undergoing single-path propagation, where $K = K_c + K_u$. The coherent signals consist of P groups. In the pth group, the coherent signal from $(\alpha_{pl}, \beta_{pl})$ due to lth multipath propagation of $s_p(t)$ with power σ_p^2 and the complex fading coefficient is ρ_{pl} with $|\rho_{pl}| \le 1, l = 1, \ldots, L_p$, $p = 1, \ldots, P$. Then the number of the coherent signals is $K_c = \sum_{p=1}^{P} L_p$, and these coherent signals can be expressed as $s_{1,1}(t), \ldots, s_{1,L_1}(t), \ldots, s_{P,1}(t), \ldots, s_{P,L_p}(t)$ where $s_{pl}(t) = \rho_{pl} s_p(t)$. The remaining incident signals are the uncorrelated ones. Without loss of generally, the signal $s_{K_c+1}(t), \ldots, s_K(t)$ are assumed to be the uncorrelated signals. The coherent signals in different groups are uncorrelated with each other. Also, the coherent signals are uncorrelated with the uncorrelated signals. Then the output of two ULAs ($\mathbf{Y}(t)$ and $\mathbf{X}(t)$) can be expressed as

$$\begin{aligned}\mathbf{Y}(t) &= \sum_{p=1}^{P}\sum_{l=1}^{L_p} \mathbf{Ca}\left(\alpha_{pl}, \beta_{pl}\right)\rho_{pl} s_p(t) \\ &\quad + \sum_{k=K_c+1}^{K} \mathbf{Ca}(\alpha_k, \beta_k) s_k(t) + \mathbf{N}_1(t) \\ &= \mathbf{CA}_c\mathbf{\Gamma}\mathbf{s}_c(t) + \mathbf{CA}_u\mathbf{s}_u(t) + \mathbf{N}_1(t) \\ &= \mathbf{CAEs}(t) + \mathbf{N}_1(t) \qquad (1)\end{aligned}$$

$$\begin{aligned}\mathbf{X}(t) &= \mathbf{CA}_c\mathbf{D}_c\mathbf{\Gamma}\mathbf{s}_c(t) + \mathbf{CA}_u\mathbf{D}_u\mathbf{s}_u(t) + \mathbf{N}_2(t) \\ &= \mathbf{CADEs}(t) + \mathbf{N}_2(t) \qquad (2)\end{aligned}$$

where $\mathbf{N}_1(t)$ and $\mathbf{N}_2(t)$ represent the $N \times 1$ additive Gaussian white noise vector with each entry equal to σ_n^2. $\mathbf{s}(t)$ is the $(P + K_u) \times 1$ signal vector given by $\mathbf{s}(t) = \left[\mathbf{s}_c^T(t), \mathbf{s}_u^T(t)\right]^T$, the coherent signal vector is represented as $\mathbf{s}_c(t) = [s_1(t), s_2(t), \ldots, s_P(t)]^T$, the uncorrelated signal vector is represented as $\mathbf{s}_u(t) = \left[s_{K_c+1}(t), s_{K_c+2}(t), \ldots, s_K(t)\right]^T$, where $(\cdot)^T$ denotes transpose. The entries of $\mathbf{s}(t)$ are zero mean wide-sense stationary random processes. $\mathbf{A} = [\mathbf{A}_c, \mathbf{A}_u]$ represents $N \times K$ array manifold matrix, where the coherent signals array manifold matrix is $\mathbf{A}_c = [\mathbf{A}_{c1}, \mathbf{A}_{c2}, \ldots, \mathbf{A}_{cP}]$, and $\mathbf{A}_{cp} = \left[\mathbf{a}\left(\alpha_{p1}\right), \mathbf{a}\left(\alpha_{p2}\right), \ldots, \mathbf{a}\left(\alpha_{pL_p}\right)\right]$, the uncorrelated signals array manifold matrix is represented as $\mathbf{A}_u = \left[\mathbf{a}\left(\alpha_{K_c+1}\right), \mathbf{a}\left(\alpha_{K_c+2}\right), \ldots, \mathbf{a}\left(\alpha_K\right)\right]$. The steering vector of the coherent signals is expressed as $\mathbf{a}\left(\alpha_{pk}\right) = \left[1, e^{j\tau(\alpha_{pk})}, \ldots, e^{j(M-1)\tau(\alpha_{pk})}\right]^T$, and the steering vector of the uncorrelated signals is expressed as $\mathbf{a}(\alpha_k) = \left[1, e^{j\tau(\alpha_k)}, \ldots, e^{j(M-1)\tau(\alpha_k)}\right]^T$. While the matrix $\mathbf{E} = blkdiag\left[\mathbf{\Gamma}, \mathbf{I}_{K_u}\right]$, and $\mathbf{\Gamma} = blkdiag\left[\boldsymbol{\rho}_1, \boldsymbol{\rho}_2, \ldots, \boldsymbol{\rho}_P\right]$, $\boldsymbol{\rho}_p = \left[\rho_{p1}, \rho_{p2}, \ldots, \rho_{pL_p}\right]^T$. The matrix $\mathbf{D} = blkdiag[\mathbf{D}_c, \mathbf{D}_u]$, where $\mathbf{D}_c = blkdiag[\mathbf{D}_{c1}, \mathbf{D}_{c2}, \ldots, \mathbf{D}_{cP}]$, and $\mathbf{D}_{cp} = diag\left[e^{j\gamma(\beta_{p1})}, e^{j\gamma(\beta_{p2})}, \ldots, e^{j\gamma\left(\beta_{pL_p}\right)}\right]$. The matrix $\mathbf{D}_u = diag\left[e^{j\gamma(\beta_{K_c+1})}, e^{j\gamma(\beta_{K_c+2})}, \ldots, e^{j\gamma(\beta_K)}\right]$. In this paper, $diag(\cdot)$, $blkdiag(\cdot)$ and $\mathbf{I}_{K_u}$ denote as the diagonal matrix, block diagonal matrix and $K_u \times K_u$ identity matrix, respectively. $\tau(\alpha) = 2\pi d_y \cos\alpha/\lambda$, and $\gamma(\beta) = 2\pi d_x \cos\beta/\lambda$.

$\mathbf{C}$ is the $N \times N$ mutual coupling matrix (MCM). The mutual coupling coefficients between two elements are inversely proportional to their distance. The mutual coupling degree of freedom is assumed to be M_0 [8]. When the distance between two elements is larger than $(M_0 - 1)d$, the mutual coupling coefficients attenuate to zero. The spacing between two ULAs is set to be $d_x = \lambda/2$. The structure of the antenna design is identical, and the elements arrangement of two ULAs is similar. For simplicity, only the mutual coupling among elements which belongs to the identical ULA is considered in this paper. Therefore, the MCM of the two ULAs can be assumed to have the same structure. i.e., the entries of the MCMs which belong to two ULAs are identical. The mutual coupling degree of freedom is assumed to be $(M_0 + 1)$, which means for the ith element, the coupling comes from the $(i - M_0)$ th to $(i + M_0)$ th elements. The MCM $\mathbf{C}$ is constructed as a banded symmetric Toeplitz matrix, whose first row is $\mathbf{c} = [1, c_1, c_2, \ldots, c_{M_0}, 0, \ldots, 0]$ satisfying $0 < |c_{M_0}| < |c_{M_0-1}| < \cdots < c_1 = 1$. The MCM $\mathbf{C}$ is given by

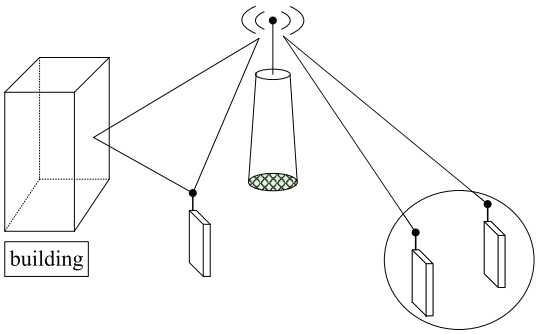

Fig. 2 DOA estimation for VMIMO scheme considering multipath propagation

$$\begin{aligned}\mathbf{C} &= Toeplitz(c)\\ &= \begin{bmatrix} 1 & c_1 & \cdots & c_{N-1} \\ c_1 & 1 & \cdots & c_{N-2} \\ \vdots & \vdots & \vdots & \vdots \\ c_{N-1} & c_{N-2} & \cdots & 1 \end{bmatrix}\\ &= \begin{bmatrix} 1 & c_1 & \cdots & c_{M_0} & \cdots & 0 \\ c_1 & 1 & c_1 & \cdots & \ddots & 0 \\ \vdots & c_1 & 1 & \ddots & \cdots & c_{M_0} \\ c_{M_0} & \cdots & \ddots & \ddots & c_1 & \vdots \\ 0 & \ddots & \cdots & c_1 & 1 & c_1 \\ 0 & \cdots & c_{M_0} & \cdots & c_1 & 1 \end{bmatrix}\end{aligned} \tag{3}$$

Based on the structure of two ULAs, some methods has been proposed without mutual coupling effects [15,19,34]. However, it is difficult to estimate 2D-DOA when the mutual coupling is not known. In the following section, a novel 2D-DOA estimation algorithm with unknown MCM $\mathbf{C}$ will be introduced.

4 2D-DOA estimation of the uncorrelated signals

In order to eliminate the effect of mutual coupling, the first and last M_0 elements of the $\bar{N} = (N - 2M_0)$-elements ULA are selected as instrumental elements in each ULA [9]. At the first glance, it is an unreasonable idea to abandon some information that the array receives. However, the effect of mutual coupling can be eliminated by this sacrifice. Define a selection matrix $\mathbf{F} = \left[\mathbf{0}_{(N-2M_0)\times M_0}\mathbf{I}_{N-2M_0}\mathbf{0}_{(N-2M_0)\times M_0}\right]$, the output of the center array is expressed as [8]

$$\begin{aligned}\bar{\mathbf{Y}}(t) &= \mathbf{F}\mathbf{Y}(t)\\ &= \mathbf{F}\mathbf{C}\mathbf{A}_c\mathbf{\Gamma}\mathbf{s}_c(t) + \mathbf{F}\mathbf{C}\mathbf{A}_u\mathbf{s}_u(t) + \mathbf{F}\mathbf{N}_1(t)\\ &= \bar{\mathbf{C}}\mathbf{A}_c\mathbf{\Gamma}\mathbf{s}_c(t) + \bar{\mathbf{C}}\mathbf{A}_u\mathbf{s}_u(t) + \bar{\mathbf{N}}_1(t)\end{aligned} \tag{4}$$

where the $\bar{M} \times M$ MCM $\bar{\mathbf{C}}$ of the center array is given by

$$\bar{\mathbf{C}} = \mathbf{F}\mathbf{C} = \begin{bmatrix} c_{M_0} & \cdots & 1 & \cdots & c_{M_0} & 0 & \cdots & 0 \\ 0 & c_{M_0} & \cdots & 1 & \cdots & c_{M_0} & \cdots & 0 \\ \vdots & \ddots & \ddots & \cdots & \ddots & \cdots & \ddots & \vdots \\ 0 & \cdots & 0 & c_{M_0} & \cdots & 1 & \cdots & c_{M_0} \end{bmatrix} \tag{5}$$

and $\bar{\mathbf{N}}_1(t) = \mathbf{F}\mathbf{N}_1(t)$. Then an important relationship between the MCM and the steering vector can be obtained, which is represented as [39]

$$\begin{aligned}\bar{\mathbf{C}}\bar{\mathbf{a}}(\alpha_k) &= \begin{bmatrix} C_1 \\ C_2 \\ \vdots \\ C_{M_0-1} \\ C_{M_0-1} \end{bmatrix} = C\begin{bmatrix} 1 \\ v_k \\ \vdots \\ v_k^{M_0-1} \end{bmatrix}\\ &= v_k^{M_0} D\bar{\mathbf{a}}(\alpha_k)\\ &= c(\alpha_k)\bar{\mathbf{a}}(\alpha_k),\end{aligned} \tag{6}$$

$$\begin{aligned}C_1 &= c_{M_0} + \cdots + c_1 v_k^{M_0-1} + v_k^{M_0}\\ &\quad + c_1 v_k^{M_0+1} + \cdots + c_{M_0} v_k^{2M_0},\\ C_2 &= c_{M_0} v_k + \cdots + c_1 v_k^{M_0} + v_k^{M_0+1}\\ &\quad + c_1 v_k^{M_0+2} + \cdots + c_{M_0} v_k^{2M_0+1},\\ C_{M_0-1} &= c_{M_0} v_k^{M-2M_0-2} + \cdots + c_1 v_k^{M-M_0-2}\\ &\quad + v_k^{M-M_0-1} + c_1 v_k^{M-M_0} + \cdots + c_{M_0} v_k^{M-2},\\ C_{M_0} &= c_{M_0} v_k^{M-2M_0-1} + \cdots + c_1 v_k^{M-M_0-1}\\ &\quad + v_k^{M-M_0} + c_1 v_k^{M-M_0+1} + \cdots + c_{M_0} v_k^{M-1},\\ C &= c_{M_0} + \cdots + c_1 v_k^{M_0-1} + v_k^{M_0}\\ &\quad + c_1 v_k^{M_0+1} + \cdots + c_{M_0} v_k^{2M_0},\\ D &= 2\sum_{m_0=1}^{M_0} c_{m_0}\cos(2m_0\pi\cos(\alpha_k)\, d/\lambda) + 1\end{aligned} \tag{7}$$

where $v_k = e^{j\tau(\alpha_k)}$ and $\bar{\mathbf{a}}(\alpha_k)$ is the ideal steering vector of the center array ($M_0 + 1 \sim M - M_0$ elements), and $c(\alpha_k)$ is a scalar function only concerned with the mutual coupling coefficients and the direction of the incident signal α_k, which is defined as

$$c(\alpha_k) = v_k^{M_0} D. \tag{8}$$

When $D \neq 0$, we have $\bar{\mathbf{C}}\mathbf{A}_c\mathbf{\Gamma} = \bar{\mathbf{A}}_c\mathbf{B}_c\mathbf{\Gamma} = \bar{\mathbf{A}}_c\bar{\mathbf{\Gamma}}$ and $\bar{\mathbf{C}}\mathbf{A}_u = \bar{\mathbf{A}}_u\mathbf{B}_u$. $\bar{\mathbf{A}}_c = \left[\bar{\mathbf{a}}_1(\alpha_1), \bar{\mathbf{a}}_2(\alpha_2), \ldots, \bar{\mathbf{a}}_{K_c}(\alpha_{K_c})\right]$ is the array manifold matrix of the centre array with respect to coherent signals. $\mathbf{B}_c = diag[\mathbf{B}_1, \mathbf{B}_2, \ldots, \mathbf{B}_P]$, $\mathbf{B}_p = diag\left[c(\alpha_{p1}), c(\alpha_{p2}), \ldots, c(\alpha_{pL_p})\right]$, and the matrix $\bar{\mathbf{\Gamma}} = blkdiag\left[\bar{\boldsymbol{\rho}}_1, \bar{\boldsymbol{\rho}}_2, \ldots, \boldsymbol{\rho}_P\right]$, where $\bar{\boldsymbol{\rho}}_{\mathbf{p}} = \mathbf{B}_p\boldsymbol{\rho}_p$. $\bar{\mathbf{A}}_u = \left[\bar{\mathbf{a}}(\alpha_{K_c+1}), \bar{\mathbf{a}}(\alpha_{K_c+2}), \ldots, \bar{\mathbf{a}}(\alpha_K)\right]$. The matrix $\mathbf{B}_u =$

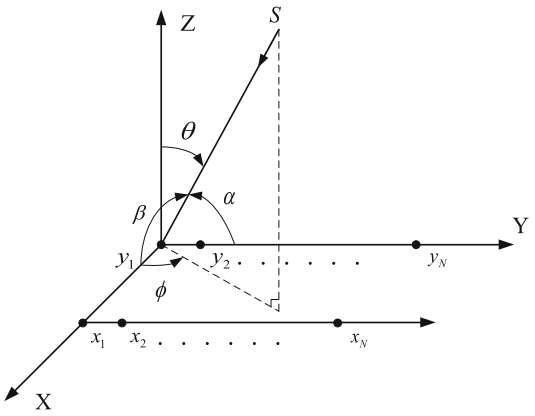

Fig. 3 The configuration of two parallel ULAs

$diag\left[c\left(\alpha_{K_c+1}\right), c\left(\alpha_{K_c+2}\right), \ldots, c\left(\alpha_K\right)\right]$. Equation (4) can be written in another form as

$$\begin{aligned}\bar{\mathbf{Y}}(t) &= \bar{\mathbf{C}}\mathbf{A}_c\boldsymbol{\Gamma}\mathbf{s}_c(t) + \bar{\mathbf{C}}\mathbf{A}_u\mathbf{s}_u(t) + \bar{\mathbf{N}}_1(t)\\ &= \bar{\mathbf{A}}_c\bar{\boldsymbol{\Gamma}}\mathbf{s}_c(t) + \bar{\mathbf{A}}_u\mathbf{B}_u\mathbf{s}_u(t) + \bar{\mathbf{N}}_1(t).\end{aligned} \tag{9}$$

In a similar way, (2) can be written as

$$\bar{\mathbf{X}}(t) = \bar{\mathbf{A}}_c\mathbf{D}_c\bar{\boldsymbol{\Gamma}}\mathbf{s}_c(t) + \bar{\mathbf{A}}_u\mathbf{B}_u\mathbf{D}_u\mathbf{s}_u(t) + \bar{\mathbf{N}}_2(t) \tag{10}$$

Based on two $\left(\bar{N}-1\right)\times\bar{N}$ selection matrices, the centre array of sub-array 1 and sub-array 2 can be divided into four arrays, which are called array 1, array 2, array 3 and array 4, respectively.

$$\mathbf{P}_1 = \begin{bmatrix} 1 & \cdots & 0 & 0\\ \vdots & \ddots & \vdots & \vdots\\ 0 & \cdots & 1 & 0\end{bmatrix}, \mathbf{P}_2 = \begin{bmatrix} 0 & 1 & \cdots & 0\\ \vdots & \vdots & \ddots & \vdots\\ 0 & 0 & \cdots & 1\end{bmatrix} \tag{11}$$

The elements $y_{M_0+1} \sim y_{N-M_0-1}$, $y_{M_0+2} \sim y_{M-M_0}$, $x_{M_0+1} \sim x_{N-M_0-1}$ and $x_{M_0+2} \sim x_{M-M_0}$ elements constitute array 1, array 2, array 3, and array 4, respectively, which can be expressed as

$$\begin{aligned}\bar{\mathbf{Y}}_1(t) &= \bar{\mathbf{A}}_{1c}\bar{\boldsymbol{\Gamma}}\mathbf{s}_c(t) + \bar{\mathbf{A}}_{1u}\mathbf{B}_u\mathbf{s}_u(t) + \bar{\mathbf{N}}_{11}(t)\\ &= \left[\bar{\mathbf{A}}_{1c}\bar{\boldsymbol{\Gamma}}, \bar{\mathbf{A}}_{1u}\mathbf{B}_u\right]\mathbf{s}(t) + \bar{\mathbf{N}}_{11}(t),\end{aligned} \tag{12}$$

$$\bar{\mathbf{Y}}_2(t) = \left[\bar{\mathbf{A}}_{1c}\mathbf{G}_c\bar{\boldsymbol{\Gamma}}, \bar{\mathbf{A}}_{1u}\mathbf{G}_u\mathbf{B}_u\right]\mathbf{s}(t) + \bar{\mathbf{N}}_{12}(t), \tag{13}$$

$$\bar{\mathbf{X}}_1(t) = \left[\bar{\mathbf{A}}_{1c}\mathbf{D}_c\bar{\boldsymbol{\Gamma}}, \bar{\mathbf{A}}_{1u}\mathbf{B}_u\mathbf{D}_u\right]\mathbf{s}(t) + \bar{\mathbf{N}}_{21}(t), \tag{14}$$

$$\bar{\mathbf{X}}_2(t) = \left[\bar{\mathbf{A}}_{1c}\mathbf{G}_c\mathbf{D}_c\bar{\boldsymbol{\Gamma}}, \bar{\mathbf{A}}_{1u}\mathbf{G}_u\mathbf{B}_u\mathbf{D}_u\right]\mathbf{s}(t) + \bar{\mathbf{N}}_{22}(t), \tag{15}$$

where the diagonal matrix $\mathbf{G} = diag\left[\mathbf{G}_c, \mathbf{G}_u\right]$, the matrix $\mathbf{G}_c = blkdiag\left[\mathbf{G}_{c1}, \mathbf{G}_{c2}, \ldots, \mathbf{G}_{cP}\right]$, and the matrix $\mathbf{G}_u = diag\left[e^{j\tau\left(\alpha_{K_c+1}\right)}, e^{j\tau\left(\alpha_{K_c+2}\right)}, \ldots, e^{j\tau\left(\alpha_K\right)}\right]$.

The auto-covariance matrix of array 1 can be represented as

$$\begin{aligned}\mathbf{R}_1 &= E\left\{\bar{\mathbf{Y}}_1(t)\bar{\mathbf{Y}}_1^H(t)\right\}\\ &= \left[\bar{\mathbf{A}}_{c1}\bar{\boldsymbol{\Gamma}}, \bar{\mathbf{A}}_{u1}\mathbf{B}_u\right]\mathbf{R}_s\left[\bar{\mathbf{A}}_{c1}\bar{\boldsymbol{\Gamma}}, \bar{\mathbf{A}}_{u1}\mathbf{B}_u\right]^H\\ &\quad + \sigma_n^2\mathbf{I}_{\bar{N}-1}\\ &= \bar{\mathbf{A}}_{c1}\bar{\boldsymbol{\Gamma}}\mathbf{R}_c\bar{\boldsymbol{\Gamma}}^H\bar{\mathbf{A}}_{c1}^H + \bar{\mathbf{A}}_{u1}\bar{\mathbf{R}}_u\bar{\mathbf{A}}_{u1}^H + \sigma_n^2\mathbf{I}_{\bar{N}-1}\\ &= \bar{\mathbf{A}}_1\bar{\mathbf{E}}\mathbf{R}_s\bar{\mathbf{E}}^H\bar{\mathbf{A}}_1^H + \sigma_n^2\mathbf{I}_{\bar{N}-1}\end{aligned} \tag{16}$$

where $\bar{\mathbf{R}}_u = \mathbf{B}_u\mathbf{R}_u\mathbf{B}_u^H$, $\mathbf{R}_s = blkdiag\left[\mathbf{R}_c, \bar{\mathbf{R}}_u\right]$ and $\bar{\mathbf{E}} = blkdiag\left[\bar{\boldsymbol{\Gamma}}, \mathbf{I}\right]$. The cross-covariance matrices can be represented as

$$\begin{aligned}\mathbf{R}_2 &= E\left\{\bar{\mathbf{Y}}_2(t)\bar{\mathbf{Y}}_1^H(t)\right\}\\ &= \bar{\mathbf{A}}_1\mathbf{G}\bar{\mathbf{E}}\mathbf{R}_s\bar{\mathbf{E}}^H\bar{\mathbf{A}}_1^H + \mathbf{R}_{n_2n_1}\end{aligned} \tag{17}$$

$$\begin{aligned}\mathbf{R}_3 &= E\left\{\bar{\mathbf{X}}_1(t)\bar{\mathbf{Y}}_1^H(t)\right\}\\ &= \bar{\mathbf{A}}_1\mathbf{D}\bar{\mathbf{E}}\mathbf{R}_s\bar{\mathbf{E}}^H\bar{\mathbf{A}}_1^H + \mathbf{R}_{n_3n_1}\end{aligned} \tag{18}$$

$$\begin{aligned}\mathbf{R}_4 &= E\left\{\bar{\mathbf{X}}_2(t)\bar{\mathbf{Y}}_1^H(t)\right\}\\ &= \bar{\mathbf{A}}_1\mathbf{G}\mathbf{D}\bar{\mathbf{E}}\mathbf{R}_s\bar{\mathbf{E}}^H\bar{\mathbf{A}}_1^H + \mathbf{R}_{n_4n_1}\end{aligned} \tag{19}$$

where the matrix $\bar{\mathbf{A}}_1 = \left[\bar{\mathbf{A}}_{c1}, \bar{\mathbf{A}}_{u1}\right]$, and the matrix $\mathbf{R}_{n_in_1} = \begin{bmatrix}\mathbf{0}_{(\bar{N}-2)\times 1} & \mathbf{I}_{\bar{N}-2}\\ \mathbf{0} & \mathbf{0}_{1\times(\bar{N}-2)}\end{bmatrix}$, $i = 1, 2, 3, 4$. The DOA matrix is defined as follows

$$\begin{aligned}\mathbf{R}_{DOA_1} &= \mathbf{R}_2\mathbf{R}_1^{\dagger},\\ \mathbf{R}_{DOA_2} &= \mathbf{R}_3\mathbf{R}_1^{\dagger},\\ \mathbf{R}_{DOA_3} &= \mathbf{R}_4\mathbf{R}_1^{\dagger}.\end{aligned} \tag{20}$$

where $(\cdot)^{\dagger}$ is the pseudo inverse of matrix $(\cdot)$. Based on the nonzero eigenvalue γ_k of $\mathbf{R}_1$ and its corresponding eigenvector u_k, $\mathbf{R}_1^{\dagger}$ can be expressed as

$$\mathbf{R}_1^{\dagger} = \sum_{k=1}^{P+K_u}\frac{1}{\gamma_k}\mathbf{u}_k\mathbf{u}_k^H. \tag{21}$$

The noise power σ_n^2 can be estimated by the $N-P-K_u$ small eigenvalues, and then the noise covariance matrices can be subtracted. The DOA-matrix can be written as

$$\begin{aligned}\mathbf{R}_{DOA_1} &= \left(\bar{\mathbf{A}}_1\mathbf{G}\bar{\mathbf{E}}\mathbf{R}_s\bar{\mathbf{E}}^H\bar{\mathbf{A}}_1^H\right)\left(\bar{\mathbf{A}}_1\bar{\mathbf{E}}\mathbf{R}_s\bar{\mathbf{E}}^H\bar{\mathbf{A}}_1^H\right)^{\dagger}\\ &= \mathbf{J}\mathbf{R}_s\bar{\mathbf{E}}^H\bar{\mathbf{A}}_1^H\\ &\quad\times\left(\bar{\mathbf{A}}_1\bar{\mathbf{E}}\mathbf{R}_s\bar{\mathbf{E}}^H\bar{\mathbf{A}}_1^H\right)^{\dagger},\\ \mathbf{J} &= \left[\bar{\mathbf{A}}_{1c1}\mathbf{G}_{c1}\bar{\boldsymbol{\rho}}_1, \bar{\mathbf{A}}_{1c2}\mathbf{G}_{c2}\bar{\boldsymbol{\rho}}_2,\right.\\ &\quad\left.\ldots, \bar{\mathbf{A}}_{1cP}\mathbf{G}_{cP}\bar{\boldsymbol{\rho}}_P, \bar{\mathbf{A}}_{u1}\mathbf{G}_u\right].\end{aligned} \tag{22}$$

According to (16), we have the matrix $\mathbf{R}_s\bar{\mathbf{E}}^H\bar{\mathbf{A}}_1^H = \left(\left(\bar{\mathbf{A}}_1\bar{\mathbf{E}}\right)^H\left(\bar{\mathbf{A}}_1\bar{\mathbf{E}}\right)\right)^{-1}\left(\bar{\mathbf{A}}_1\bar{\mathbf{E}}\right)^H\mathbf{R}_1$. Then (17) can be written

as

$$\mathbf{R}_2 = \bar{\mathbf{A}}_1\mathbf{G}\bar{\mathbf{E}}\left(\left(\bar{\mathbf{A}}_1\bar{\mathbf{E}}\right)^H\left(\bar{\mathbf{A}}_1\bar{\mathbf{E}}\right)\right)^{-1}\left(\bar{\mathbf{A}}_1\bar{\mathbf{E}}\right)^H\mathbf{R}_1 + \mathbf{R}_{n_2n_1} \tag{23}$$

Based on Lemma 1 of [41], the relationship among $\bar{\mathbf{A}}_1$,$\mathbf{G}$, $\mathbf{R}_{DOA_1}$ and $\bar{\mathbf{E}}$ is given by

$$\mathbf{R}_{DOA_1}\bar{\mathbf{A}}_{1cp}\bar{\boldsymbol{\rho}}_p = \bar{\mathbf{A}}_{1cp}\mathbf{G}_{cp}\bar{\boldsymbol{\rho}}_p,\ p = 1, 2, \ldots, P \tag{24}$$

$$\mathbf{R}_{DOA_1}\bar{\mathbf{A}}_{1u} = \bar{\mathbf{A}}_{1u}\mathbf{G}_u. \tag{25}$$

It can be seen from (25) that K_u diagonal elements of $\mathbf{G}_u$ are a part of the nonzero eigenvalues of $\mathbf{R}_{DOA_1}$. The rank of $\mathbf{R}_{DOA_1}$ is $K_u + P$, the remaining P eigenvalues are related to the D groups of coherent signals from (24). According to the similar derivation of $\mathbf{R}_{DOA_1}$, $\mathbf{R}_{DOA_2}$ and R_{DOA_3} have the similar property as $\mathbf{R}_{DOA_1}$, which are given by

$$\mathbf{R}_{DOA_2}\bar{\mathbf{A}}_{2cp}\bar{\boldsymbol{\rho}}_p = \bar{\mathbf{A}}_{2cp}\mathbf{D}_{cp}\bar{\boldsymbol{\rho}}_p,\ p = 1, 2, \ldots, P \tag{26}$$

$$\mathbf{R}_{DOA_2}\bar{\mathbf{A}}_{2u} = \bar{\mathbf{A}}_{2u}\mathbf{D}_u. \tag{27}$$

$$\mathbf{R}_{DOA_3}\bar{\mathbf{A}}_{3cp}\bar{\boldsymbol{\rho}}_p = \bar{\mathbf{A}}_{3cp}\mathbf{G}_{cp}\mathbf{D}_{cp}\bar{\boldsymbol{\rho}}_p,\ p = 1, 2, \ldots, P \tag{28}$$

$$\mathbf{R}_{DOA_3}\bar{\mathbf{A}}_{3u} = \bar{\mathbf{A}}_{3u}\mathbf{G}_u\mathbf{D}_u. \tag{29}$$

By taking eigen-decomposition, $\mathbf{R}_{DOA_1}$ can be written as

$$\mathbf{R}_{DOA_1} = \mathbf{U}_1\boldsymbol{\Lambda}_1\mathbf{U}_1^{-1} \tag{30}$$

where $\boldsymbol{\Lambda}_1 = diag\left[\delta_{11}, \delta_{12}, \ldots, \delta_{1(K_u+P)}\right]$ stands for the eigenvalues of $\mathbf{R}_{DOA_1}$ and their corresponding eigenvectors are $\mathbf{U}_1 = \left[\mathbf{u}_{11}, \mathbf{u}_{12}, \ldots, \mathbf{u}_{1(K_u+P)}\right]$. Because $\bar{\mathbf{A}}_{1cp}$, $p = 1, 2, \ldots, P$ are Vandermonde matrices, we can not obtain another steering vector based on the combination of the steering vectors. The coherent signals do not have the characteristic that the uncorrelated signals have, and the characteristic is shown in (25). The moduli of the eigenvalues which belong to the uncorrelated signals are equal to 1. However, the moduli of the eigenvalues which belong to the coherent signals are not equal to 1 [13]. This property can be used to distinguish the uncorrelated and coherent signals. Based on (30), $\mathbf{R}_{DOA_2}$ and $\mathbf{R}_{DOA_3}$ can be written as

$$\mathbf{R}_{DOA_2} = \mathbf{U}_2\boldsymbol{\Lambda}_2\mathbf{U}_2^{-1} \tag{31}$$

$$\mathbf{R}_{DOA_3} = \mathbf{U}_3\boldsymbol{\Lambda}_3\mathbf{U}_3^{-1} \tag{32}$$

where the matrix $\boldsymbol{\Lambda}_2 = diag\left[\delta_{21}, \delta_{22}, \ldots, \delta_{2(K_u+P)}\right]$, and the matrix $\boldsymbol{\Lambda}_3 = diag\left[\delta_{31}, \delta_{32}, \ldots, \delta_{3(K_u+P)}\right]$ are the eigenvalues of $\mathbf{R}_{DOA_2}$ and $\mathbf{R}_{DOA_3}$, respectively. The matrix $\mathbf{U}_2 = \left[\mathbf{u}_{21}, \mathbf{u}_{22}, \ldots, \mathbf{u}_{2(K_u+P)}\right]$ and the matrix $\mathbf{U}_3 = \left[\mathbf{u}_{31}, \mathbf{u}_{32}, \ldots, \mathbf{u}_{3(K_u+P)}\right]$ are the corresponding eigenvectors. However, when $P \geq 2$, the eigen-decomposition of $\mathbf{R}_{DOA_2}$ and $\mathbf{R}_{DOA_3}$ are taken separately, thus the parameter pairing between $\delta_{11}, \delta_{12}, \ldots, \delta_{1(K_u+P)}$ and $\delta_{21}, \delta_{22}, \ldots, \delta_{2(K_u+P)}$ is a big problem. According to (24)–(29), we can know that $\boldsymbol{\Lambda}_3 = \boldsymbol{\Lambda}_2\boldsymbol{\Lambda}_1$. Thus the parameter pairing problem can be transformed as a problem which minimizes (33)

$$\min\left|angle\left(\delta_{3k}\right) - \left[angle\left(\delta_{1i}\right) + angle\left(\delta_{2j}\right)\right]\right| \tag{33}$$

Then parameter pairing is accomplished. The 2D-DOA of the uncorrelated signals can be represented as

$$\begin{aligned}\alpha_k &= \arccos\left(\frac{\lambda}{2\pi d_y}\left[angle\left(\delta_{1k}\right) + angle\left(\frac{\delta_{3k}}{\delta_{2k}}\right)\right]\right),\\ \beta_k &= \arccos\left(\frac{\lambda}{2\pi d_x}\left[angle\left(\delta_{2i}\right)\right] + angle\left(\frac{\delta_{3k}}{\delta_{1k}}\right)\right),\\ k &= 1, 2, \ldots, K_u\end{aligned} \tag{34}$$

5 The Mutual coupling coefficients estimation

Based on the 2D-DOA estimation of the uncorrelated signals, the estimations of mutual coupling coefficients can be obtained. The covariance matrix of $\mathbf{Y}(t)$ can be expressed as

$$\begin{aligned}\mathbf{R}_Y &= E\left\{\mathbf{Y}(t)\mathbf{Y}^H(t)\right\}\\ &= \mathbf{CAER}_s\mathbf{E}^H\mathbf{A}^H\mathbf{C}^H + \sigma_n^2\mathbf{I}_N\\ &= \mathbf{CA}_c\boldsymbol{\Gamma}\mathbf{R}_c\boldsymbol{\Gamma}^H\mathbf{A}_c^H\mathbf{C}^H + \mathbf{CA}_u\mathbf{R}_u\mathbf{A}_u^H\mathbf{C}^H\\ &\quad + \sigma_n^2\mathbf{I}_N.\end{aligned} \tag{35}$$

The rank of $\mathbf{CAER}_s\mathbf{E}^H\mathbf{A}^H\mathbf{C}^H$ is $K_u + P$. Take the eigen-decomposition of $\mathbf{R}_Y$, the $K_u + P$ big eigenvalues $\lambda_1, \lambda_2, \ldots, \lambda_{K_u+P}$ and $K - (K_u + P)$ small eigenvalues $\lambda_{K_u+P+1} = \lambda_{K_u+P+2} = \cdots = \lambda_K = \sigma_n^2$ can be obtained, respectively. Their corresponding eigenvectors are $\mathbf{u}_1, \mathbf{u}_2, \ldots, \mathbf{u}_M$. The signal subspace is spanned by $\mathbf{CA}_c$ and $\mathbf{CA}_u$ jointly, which is orthogonal to the noise subspace spanned by $\mathbf{u}_{K_u+P+1}, \mathbf{u}_{K_u+P+2}, \ldots, \mathbf{u}_M$

$$\begin{aligned}&\mathbf{U}_n^H\mathbf{CA}_{cp}\boldsymbol{\rho}_p = 0,\ p = 1, 2, \ldots, P\\ &\mathbf{U}_n^H\mathbf{Ca}(\alpha_k) = 0, k = 1, 2, \ldots, K_u.\end{aligned} \tag{36}$$

By considering the complex symmetric Toeplitz form of $\mathbf{C}$, $\mathbf{Ca}(\alpha)$ can be expressed as [22]

$$\begin{aligned}\mathbf{Ca}(\alpha) &= \begin{bmatrix}1 & c_1 & \cdots & c_{N-1}\\ c_1 & 1 & \cdots & c_{N-2}\\ \vdots & \vdots & \vdots & \vdots\\ c_{N-1} & c_{N-2} & \cdots & 1\end{bmatrix}\begin{bmatrix}1\\ e^{j\tau(\alpha)}\\ \vdots\\ e^{j(N-1)\tau(\alpha)}\end{bmatrix}\\ &= \begin{bmatrix}1 & e^{j\tau(\alpha)}\\ e^{j\tau(\alpha)} & 1 + e^{j2\tau(\alpha)}\\ e^{j2\tau(\alpha)} & e^{j\tau(\alpha_k)} + e^{j3\tau(\alpha)}\\ \vdots & \vdots\\ e^{j(N-2)\tau(\alpha)} & e^{j(N-3)\tau(\alpha)} + e^{j(N-1)\tau(\alpha)}\\ e^{j(N-1)\tau(\alpha)} & e^{j(N-2)\tau(\alpha)}\end{bmatrix}\end{aligned}$$

$$\begin{aligned}
&\begin{bmatrix}
\cdots & e^{j(N-2)\tau(\alpha)} & e^{j(N-1)\tau(\alpha)} \\
\cdots & e^{j(N-1)\tau(\alpha)} & 0 \\
\cdots & 0 & 0 \\
\ddots & \vdots & 0 \\
\cdots & 1 & 0 \\
\cdots & e^{j\tau(\alpha)} & 1
\end{bmatrix}
\begin{bmatrix}
1 \\ c_1 \\ \vdots \\ c_{N-1}
\end{bmatrix} \\
&= \mathbf{T}(\alpha)\,\mathbf{c}
\end{aligned} \tag{37}$$

where $\mathbf{T}(\alpha)$ is the sum of two $N \times (M_0+1)$ [12].

Based on (35) and the estimations of $\alpha_1, \alpha_2, \ldots, \alpha_{K_u}$, we have

$$\mathbf{U}_n^H \mathbf{T}(\alpha_k)\,\mathbf{c} = 0,\ k = 1, 2, \ldots, K_u \tag{38}$$

It can be seen that (38) is the linear equations of mutual coupling coefficients $\mathbf{c}$. The coefficient matrix can be defined as [37]

$$\mathbf{Q} = \begin{bmatrix} \mathbf{U}_n^H \mathbf{T}(\alpha_1) \\ \vdots \\ \mathbf{U}_n^H \mathbf{T}\left(\alpha_{K_u}\right) \end{bmatrix}. \tag{39}$$

Then (38) can be written as

$$\mathbf{Q}\mathbf{c} = 0, \tag{40}$$

where $\mathbf{Q}$ is a $K_u(N-K_u-P) \times (M_0+1)$ matrix, $\mathbf{Q} = \left[\mathbf{q}_1, \mathbf{q}_2, \ldots, \mathbf{q}_{K_u}\right]$. Due to $\mathbf{c}(1) = 1$, we have

$$\mathbf{Q}\mathbf{c} = \left[\mathbf{q}_1, \mathbf{q}_2, \ldots, \mathbf{q}_{M_0+1}\right] \begin{bmatrix} 1 \\ c_1 \\ \vdots \\ c_{M_0} \end{bmatrix} = 0. \tag{41}$$

When $K_u(N-K_u-P) \geq M_0 - 1$, the least square solution is obtained as [39]

$$\left[c_1, c_2, \ldots, c_{M_0}\right] = -\left[\mathbf{q}_2, \ldots, \mathbf{q}_{M_0+1}\right]^{\dagger} \mathbf{q}_1. \tag{42}$$

The mutual coupling coefficients estimation is completed.

6 2D-DOA estimation of the coherent signals

In order to estimate the DOA of coherent signals, the information of uncorrelated signals has to be eliminated from the covariance matrix of the array output. The DOA estimation of coherent signals can be accomplished by the reduced array. However, the loss of array aperture exists. In order to solve this problem, the original array is used here. The uncorrelated signal steering matrix $\mathbf{A}_u$ and the MCM $\mathbf{C}$ can be constructed by the estimates of $\alpha_1, \ldots, \alpha_{K_u}$ and $c_1, c_2, \ldots, c_{M_0}$, respectively. Based on the oblique projection technique, the information of coherent signals can be separated from uncorrelated signals. Then an $N \times N$ oblique projection operator $\mathbf{P}$ can be defined as [37]

$$\mathbf{P} = \mathbf{C}\mathbf{A}_u \left(\mathbf{A}_u^H \mathbf{C}^H \mathbf{P}^{\perp}_{\mathbf{C}\mathbf{A}_c\boldsymbol{\Gamma}} \mathbf{C}\mathbf{A}_u\right)^{-1} \mathbf{A}_u^H \mathbf{C}^H \mathbf{P}^{\perp}_{\mathbf{C}\mathbf{A}_c\boldsymbol{\Gamma}} \tag{43}$$

where $\mathbf{P}^{\perp}_{\mathbf{C}\mathbf{A}_c\boldsymbol{\Gamma}}$ stands for the orthogonal complement space spanned by the column of $\mathbf{C}\mathbf{A}_c\boldsymbol{\Gamma}$. The oblique projection operator $\mathbf{P}$ is difficult to obtain without $\mathbf{A}_c$. Then an alternative method for computation of oblique projector is used here [30]. The cross-covariance matrix between $\mathbf{Y}(t)$ and $\mathbf{X}(t)$ is expressed as

$$\begin{aligned}
\mathbf{R}_{XY} &= E\left\{\mathbf{X}(t)\,\mathbf{Y}^H(t)\right\} \\
&= \mathbf{C}\mathbf{A}_c \mathbf{D}_c \boldsymbol{\Gamma} \mathbf{R}_c \boldsymbol{\Gamma}^H \mathbf{A}_c^H \mathbf{C}^H \\
&\quad + \mathbf{C}\mathbf{A}_u \mathbf{D}_u \mathbf{R}_u \mathbf{A}_u^H \mathbf{C}^H.
\end{aligned} \tag{44}$$

Then the oblique projector computation method for $\mathbf{R}_{XY}$ is introduced as follows. A new $N \times N$ matrix is defined as

$$\begin{aligned}
\mathbf{R}_e &= \mathbf{R}_{XY} \mathbf{P}^{\perp}_{\mathbf{C}\mathbf{A}_u} \\
&= \mathbf{C}\mathbf{A}_c \mathbf{D}_c \boldsymbol{\Gamma} \mathbf{R}_c \boldsymbol{\Gamma}^H \mathbf{A}_c^H \mathbf{C}^H \mathbf{P}^{\perp}_{\mathbf{C}\mathbf{A}_u}
\end{aligned} \tag{45}$$

where $\mathbf{P}^{\perp}_{\mathbf{C}\mathbf{A}_u} = \mathbf{I}_N - \mathbf{C}\mathbf{A}_u \left((\mathbf{C}\mathbf{A}_u)^H \mathbf{C}\mathbf{A}_u\right)^{-1} (\mathbf{C}\mathbf{A}_u)^H$. Obviously the rank of the matrix $\mathbf{R}_e$ is $\mathbf{P}$, its QR decomposition is expressed as

$$\begin{aligned}
\mathbf{R}_e \boldsymbol{\Pi} &= \mathbf{Q}\tilde{\mathbf{R}} \\
&= \left[\tilde{\mathbf{q}}_1, \tilde{\mathbf{q}}_2, \ldots, \tilde{\mathbf{q}}_N\right] \begin{bmatrix} \tilde{\mathbf{R}}_1 \\ \mathbf{0}_{(N-P)\times N} \end{bmatrix} = \tilde{\mathbf{Q}}_1 \tilde{\mathbf{R}}_1
\end{aligned} \tag{46}$$

where the matrix $\tilde{\mathbf{Q}}_1 = \left[\tilde{\mathbf{q}}_1, \tilde{\mathbf{q}}_2, \ldots, \tilde{\mathbf{q}}_P\right]$, the matrix $\tilde{\mathbf{Q}}_2 = \left[\tilde{\mathbf{q}}_{P+1}, \tilde{\mathbf{q}}_{P+2}, \ldots, \tilde{\mathbf{q}}_N\right]$ and $\tilde{\mathbf{Q}} = \begin{bmatrix} \tilde{\mathbf{Q}}_1 & \tilde{\mathbf{Q}}_2 \end{bmatrix}$ is a $N \times N$ unitary matrix. $\tilde{\mathbf{R}}_1$ is a $P \times N$ full row rank matrix and $\boldsymbol{\Pi}$ is a permutation matrix. Referring to the conclusion in [30], the alternative computation of the oblique projector can be obtained as follows

$$\mathbf{P}_{XY} = \mathbf{C}\mathbf{A}_u \left(\tilde{\mathbf{Q}}_2 \tilde{\mathbf{Q}}_2^H \mathbf{C}\mathbf{A}_u\right)^{\dagger}. \tag{47}$$

Then the matrix $\tilde{\mathbf{H}}_{XY}$ that does not contain the information of the uncorrelated signals is expressed as

$$\begin{aligned}
\tilde{\mathbf{H}}_{XY} &= (\mathbf{I} - \mathbf{P}_{XY})\,\mathbf{R}_{XY} \\
&= \mathbf{C}\mathbf{A}_c \mathbf{D}_c \boldsymbol{\Gamma} \mathbf{R}_c \boldsymbol{\Gamma}^H \mathbf{A}_c^H \mathbf{C}^H
\end{aligned} \tag{48}$$

Another method of the oblique projector computation for $\mathbf{R}_Y$ is introduced as follows. Referring to the derivation in [36], when $K_u + P \leq N$, the oblique projector computation method is given by

$$\mathbf{P}_Y = \mathbf{C}\mathbf{A}_u \left(\mathbf{A}_u^H \mathbf{C}^H \mathbf{R}_Y^{\dagger} \mathbf{C}\mathbf{A}_u\right)^{-1} \mathbf{A}_u^H \mathbf{C}^H \mathbf{R}_Y^{\dagger}. \tag{49}$$

Similar as $\tilde{\mathbf{H}}_{XY}$, $\tilde{\mathbf{H}}_{Y}$ is expressed as

$$\tilde{\mathbf{H}}_{Y} = (\mathbf{I} - \mathbf{P}_{Y})\,\mathbf{R}_{Y} = \mathbf{C}\mathbf{A}_{c}\boldsymbol{\Gamma}\mathbf{R}_{c}\boldsymbol{\Gamma}^{H}\mathbf{A}_{c}^{H}\mathbf{C}^{H}. \tag{50}$$

In order to eliminate the effect of mutual coupling, we can multiply $\mathbf{C}^{-1}$ on both sides of $\tilde{\mathbf{H}}_{XY}$ and $\tilde{\mathbf{H}}_{Y}$. Then $\tilde{\mathbf{R}}_{XY}$ and $\tilde{\mathbf{R}}_{Y}$ can be obtained which are expressed as

$$\tilde{\mathbf{R}}_{XY} = \mathbf{C}^{-1}\mathbf{R}_{XY}\left(\mathbf{C}^{-1}\right)^{H} = \mathbf{A}_{c}\mathbf{D}_{c}\boldsymbol{\Gamma}\mathbf{R}_{c}\boldsymbol{\Gamma}^{H}\mathbf{A}_{c}^{H}, \tag{51}$$

$$\tilde{\mathbf{R}}_{Y} = \mathbf{C}^{-1}\mathbf{R}_{Y}\left(\mathbf{C}^{-1}\right)^{H} = \mathbf{A}_{c}\boldsymbol{\Gamma}\mathbf{R}_{c}\boldsymbol{\Gamma}^{H}\mathbf{A}_{c}^{H}. \tag{52}$$

Based on (51) and (52), the spatial smoothing is performed on $\tilde{\mathbf{R}}_{XY}$ and $\tilde{\mathbf{R}}_{Y}$, respectively. Notice that the smoothing here is only based on mathematical submatrices and not on real subarrays. The size of subarrays is assumed to be M_1, and the number of subarrays is $L = N - M_1 + 1$. The submatrices can be equivalent to the covariance matrices of some overlapped subarrays, which are expressed as

$$\tilde{\mathbf{R}}_{XY}^{l} = \tilde{\mathbf{R}}_{XY}\,(l : l + N - 1, l : l + N - 1)\,, \tag{53}$$

$$\tilde{\mathbf{R}}_{Y}^{l} = \tilde{\mathbf{R}}_{Y}\,(l : l + N - 1, l : l + N - 1)\,. \tag{54}$$

The smoothed auto-covariance matrix $\bar{\mathbf{R}}_{Y}^{l}$ can be obtained

$$\bar{\mathbf{R}}_{Y} = \frac{1}{N - M_1 + 1}\sum_{l=1}^{N-M_1+1}\tilde{\mathbf{R}}_{Y}^{l} = \mathbf{A}_{sub1}\bar{\mathbf{R}}_{s}\mathbf{A}_{sub1}^{H} \tag{55}$$

where $\mathbf{A}_{sub1}$ is the array manifold matrix of the first equivalent subarray and $\bar{\mathbf{R}}_{s}$ is covariance matrix of the coherent signals, which is given by

$$\bar{\mathbf{R}}_{s} = \frac{1}{N - M_1 + 1}\sum_{l=1}^{N-M_1+1}\mathbf{G}_{c}\boldsymbol{\Gamma}\mathbf{R}_{c}\boldsymbol{\Gamma}^{H}\mathbf{G}_{c}^{H}. \tag{56}$$

The smoothed cross-covariance matrix $\bar{\mathbf{R}}_{XY}^{l}$ can be obtained

$$\begin{aligned}\bar{\mathbf{R}}_{XY} &= \frac{1}{N - M_1 + 1}\sum_{l=1}^{N-M_1+1}\tilde{\mathbf{R}}_{XY}^{l} \\ &= \mathbf{A}_{sub1}\mathbf{D}_{c}\bar{\mathbf{R}}_{s}\mathbf{A}_{sub1}^{H}.\end{aligned} \tag{57}$$

The DOA-matrix is redefined as follows

$$\bar{\mathbf{R}}_{DOA} = \bar{\mathbf{R}}_{XY}\left(\bar{\mathbf{R}}_{Y}\right)^{\dagger}. \tag{58}$$

The eigen-decomposition is taken on $\bar{\mathbf{R}}_{DOA}$, we have

$$\bar{\mathbf{R}}_{DOA} = \mathbf{U}_{c}\boldsymbol{\Lambda}_{c}\mathbf{U}_{c}^{-1}, \tag{59}$$

where $\boldsymbol{\Lambda}_{c} = diag\left[\delta_{c1}, \delta_{c2}, \ldots, \delta_{cK_u}\right]$ stands for the eigenvalues of $\bar{\mathbf{R}}_{DOA}$ and their corresponding eigenvectors are $\mathbf{U}_{c} = \left[\mathbf{u}_{c1}, \mathbf{u}_{c2}, \ldots, \mathbf{u}_{cK_u}\right]$. Then $\alpha_1, \ldots, \alpha_{K_c}$ and $\beta_1, \ldots, \beta_{K_c}$ can be obtained.

$$\begin{aligned}\alpha_k &= \arccos T \\ T &= \left(\frac{\lambda}{2\pi d_x(M_1-1)}\sum_{i=2}^{M_1}\frac{1}{i-1}\left[angle\left|\frac{\mathbf{u}_{ck}(i)}{\mathbf{u}_{ck}(1)}\right|\right]\right), \\ \beta_k &= \arccos\left(\frac{\lambda}{2\pi d_y}angle\,(\delta_{ck})\right), k = 1, 2, \ldots, K_c\end{aligned} \tag{60}$$

where $\mathbf{u}_{ck}\,(i)$ stands for the ith element of the eigenvector $\mathbf{u}_{ck}$.

When the 2D-DOAs of all the incident signals are obtained, they can also be converted to the azimuth and elevation as $\phi = \arctan(\cos\beta/\cos\alpha)$ and $\varphi = \arccos\sqrt{(\cos\alpha)^2 + (\cos\beta)^2}$, respectively.

7 Summary of the algorithm and discussions

In this section, the steps of the proposed algorithm are summarized at first. Then the minimum acquired number of elements is analyzed. The steps of the proposed algorithm are summarized as follows.

Step 1: Based on the selection matrix $\mathbf{F}$, the effect of MCM is eliminated. The output of the center array are expressed as $\bar{\mathbf{Y}}\,(t)$ and $\bar{\mathbf{X}}\,(t)$, respectively.

Step 2: The centre array of sub-array 1 and sub-array 2 are divided into four arrays. The output of these arrays are $\bar{\mathbf{Y}}_1\,(t)$ $\bar{\mathbf{Y}}_2\,(t)$ and $\bar{\mathbf{X}}_1\,(t)$, $\bar{\mathbf{X}}_2\,(t)$, $t = 1, 2, \ldots, N_p$ which are called array 1, array 2, array 3 and array 4, respectively. N_p is the snapshot number. The estimate of $\mathbf{R}_1$ is expressed as

$$\hat{\mathbf{R}}_{1} = \frac{1}{N_p}\sum_{t=1}^{N_p}\bar{\mathbf{Y}}_1\,(t)\,\bar{\mathbf{Y}}_1\,(t)^{H}. \tag{61}$$

Then the estimates of $\mathbf{R}_2$, $\mathbf{R}_3$, $\mathbf{R}_4$ can be obtained in the similar way. The estimates $\hat{\mathbf{R}}_{DOA_1}$, $\hat{\mathbf{R}}_{DOA_2}$ and $\hat{\mathbf{R}}_{DOA_3}$ of DOA matrix $\mathbf{R}_{DOA_1}$, $\mathbf{R}_{DOA_2}$ and $\mathbf{R}_{DOA_3}$ can be obtained respectively.

Step 3: The eigen decomposition is taken on $\hat{\mathbf{R}}_{DOA_1}$, $\hat{\mathbf{R}}_{DOA_2}$ and $\hat{\mathbf{R}}_{DOA_3}$, respectively. The parameter pairing between azimuth and elevation can be accomplished based on (33). The 2D-DOA of uncorrelated signals can be separated from the mixed signals by the judgment criterion in Section 3. Based on (34), the 2D-DOA estimation of the uncorrelated signals is completed.

Step 4: The orthogonality between signal subspace and noise subspace is used for mutual coupling coefficients estimation. In order to construct the linear equations (40) of mutual coupling coefficients c, the form of $\mathbf{Ca}\,(\alpha)$ is changed. Based on (42), the mutual coupling coefficients estimation is accomplished.

Step 5: Based on (47) and (49), the oblique projection technique is used. the information of coherent signals can be separated from uncorrelated signals.

Step 6: Perform eigen-decomposition on $\bar{\mathbf{R}}_{DOA}$ (59) to resolve the coherent signals as in (60).

As mentioned above, the 2D-DOAs of uncorrelated and coherent signals are estimated separately. Then the uncorrelated and the coherent signals coming from the same direction can be distinguished by this two stage process. More signals than array sensors can be resolved. The proposed algorithm can estimate 2D-DOA in parallel, which is suitable for practical application. In the following, the required number of elements for DOA estimation will be analyzed.

In order to eliminate the effect of mutual coupling, only $N - 2M_0$ elements can be used for estimating uncorrelated signals. The sub-array 1 and sub-array 2 both contain $N - 2M_0 - 1$ elements. The number of sub-array has to be satisfied $N - 2M_0 - 1 \geq K_u + P + 1$. There needs $N \geq K_u + P + 2M_0 + 2$ to estimate uncorrelated signals. In order to estimate mutual coupling coefficients, $K_u (N - K_u - P) \geq M_0 - 1$ is necessary. Thus $N \geq K_u + P + \left\lceil \frac{M_0 - 1}{K_u} \right\rceil$. In order to estimate coherent signals, $N - L + 1 \geq K_c + 1$ and $L \geq \max(L_1, L_2, \ldots L_P) = L_{\max}$ are needed. $N \geq K_c + L_{\max}$ has to be satisfied. Thus the required number of elements for DOA estimation is $N \geq \max(K_u + P + 2M_0 + 2, K_c + L_{\max})$.

There is another phenomenon called "blind angles", which means the array is blind which can not receive any incident signal from some particular angles [39]. These angles make $D = 0$. Then whenever there is one incident signal with its DOA $\alpha_j = \alpha_k, k = 1, 2, \ldots, K_u.$, the array output of the center $N - 2M_0$ elements can be represented as

$$\begin{aligned}\mathbf{Y}(t) &= \sum_{p=1}^{P} \sum_{l=1}^{L_p} \bar{\mathbf{C}}\mathbf{a}\left(\alpha_{pl}, \beta_{pl}\right) \rho_{pl} s_p(t) \\ &\quad + \sum_{k=K_c+1}^{K} \bar{\mathbf{C}}\mathbf{a}(\alpha_k, \beta_k) s_k(t) + \bar{\mathbf{N}}_1(t) \\ &= \sum_{p=1}^{P} \sum_{l=1}^{L_p} \bar{\mathbf{C}}\mathbf{a}\left(\alpha_{pl}, \beta_{pl}\right) \rho_{pl} s_p(t) \\ &\quad + \sum_{k=K_c+1, j\neq k}^{K} \bar{\mathbf{C}}\mathbf{a}(\alpha_k, \beta_k) s_k(t) + \bar{\mathbf{N}}_1(t)\end{aligned}$$

The equation above implies that the jth incident signal is not contained. So at some particular angles, the array is blind which can not receive any incident signal from these directions. Thus the estimated angles of the uncorrelated signals would be lost. The number of the lost angles can be estimated by the difference in the large eigenvalues between $\mathbf{R}_Y$ and $\mathbf{R}_1$. The number of the lost angles is assumed to be K_0, so only $K_u - K_0$ uncorrelated signals are estimated. Fortunately, the lost angle can be found back in the estimation of coherent signals. When $N \geq K_u + P + \left\lceil \frac{M_0 - 1}{K_u - K_0} \right\rceil$, the uncorrelated signal steering matrix, the MCM and the oblique projection operator $\mathbf{P}$ can be constructed by the $K_u - K_0$ estimators. The remaining K_0 DOA of uncorrelated signals will be contained in (56). The K_0 lost angles of uncorrelated signals and K_c coherent signals can be estimated together [37].

8 The simulation results

In this section, simulations are shown to demonstrated properties of the proposed algorithm. The method of FBSS proposed in [31] combined with the DOA-matrix method and CRB are used as the comparison. Each ULA of the parallel-shaped array has twelve elements. The spacing of elements d_y and the spacing between two ULAs d_x are equivalent with half-wavelength ($d_y = d_x = \lambda/2$). 500 Monte Carlo trials are taken from the simulation. The average root mean square error (RMSE) is defined as

$$RMSE = \sqrt{\frac{1}{500I} \sum_{m=1}^{500} \sum_{k=1}^{I} \left(\hat{\alpha}_k(m) - \alpha_k\right)^2 + \left(\hat{\beta}_k(m) - \beta_k\right)^2} \tag{62}$$

$$RMSE_c = \sqrt{\frac{1}{500 \|\mathbf{c}_1\|} \sum_{m=1}^{500} \left\|\hat{\mathbf{c}}_1(m) - \mathbf{c}_1\right\|} \times 100\ \% \tag{63}$$

where $\hat{\alpha}_k(m)$, $\hat{\beta}_k(m)$ and $\hat{\mathbf{c}}_1(m)$ are the estimates of α_k, β_k and $\mathbf{c}_1$ of the mth Monte Carlo trials, respectively. I is the number of all the uncorrelated signals or all the coherent signals. $\|\cdot\|$ is defined as the Frobenius norm. The uncorrelated and coherent signals of the proposed algorithm can be estimated separately. In this comparison, the FBSS method has to estimate the uncorrelated and coherent signals together, the same method of eliminating the mutual coupling is used.

Five incident signals with equal power come from the direction $(100°, 60°)$, $(75°, 30°)$, $(86°, 53°)$, $(76°, 67°)$, $(16°, 83°)$, and without loss of generality the first two signals are coherent signals, and the fading coefficients are $[1, 0.7415 - \mathrm{j}0.5100]$. The last three signals are uncorrelated signals. The mutual coupling coefficients are $[1, \mathrm{j}0.4499 - 0.5362]$. In Sect. 5, the size of subarrays is $M_1 = 7$. The number of snapshot is 500. The RMSE of the DOA estimation of uncorrelated and coherent signals versus input SNR is shown in Figs. 4 and 5, respectively.

For the uncorrelated signals, it can be seen from Fig. 4 that the DOA estimation errors of the two algorithms reduce with the SNR increases. The DOA estimation performance of proposed algorithm outperforms than that of the FBSS algorithm. The azimuth estimation RMSE of the proposed algorithm approximates to the CRB at low SNR. Both the two algorithms approximate to the CRB at high SNR. For the coherent signals, it can be seen from Fig. 5 that the RMSE of FBSS algorithm changes very little with the varying

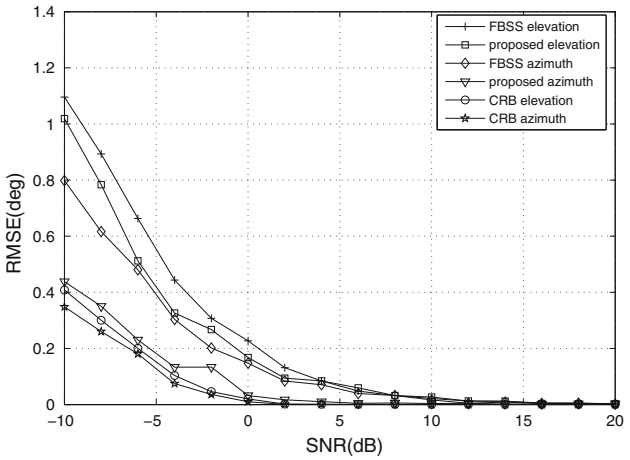

Fig. 4 RMSE of DOA estimations versus input SNR for uncorrelated signal

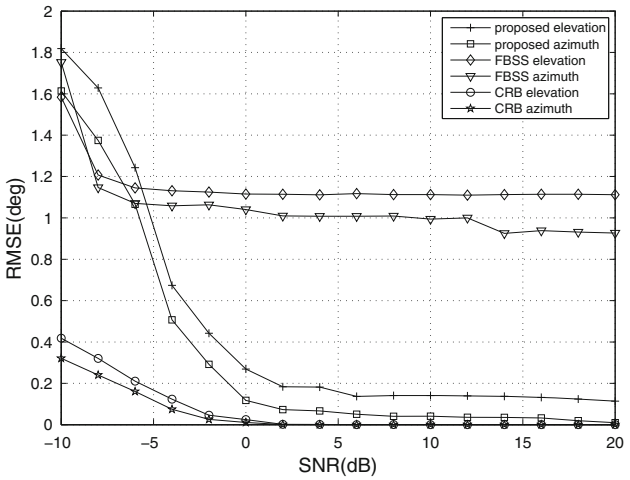

Fig. 5 RMSE of DOA estimations versus input SNR for coherent signal

SNR. However, the RMSE of the proposed algorithm reduces with SNR increases. The RMSE of the proposed algorithm approximates to the CRB at high SNR. This result is mainly caused that the proposed algorithm estimates the uncorrelated signals and the coherent signals separately. However, the FBSS algorithm estimates both the signals simultaneously. The mutual coupling estimation versus input SNR is shown in Fig. 6. The results show that the mutual coupling has little influence on the proposed algorithm. Although some array apertures are used to eliminate the effect of mutual coupling, the proposed algorithm still has high estimation accuracy and approaches to CRB at high SNR.

9 Conclusions

In this paper, the VMIMO scheme for DOA estimation is introduced which replaces the sequential scheme. It means

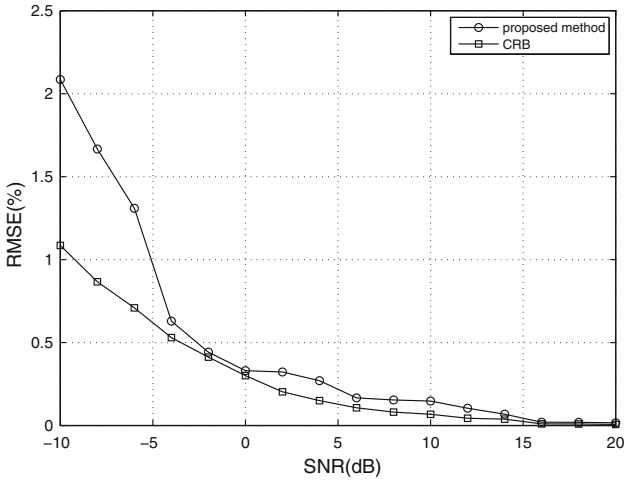

Fig. 6 RMSE of the mutual coupling coefficients versus input SNR

that the BS can detect the 2D-DOA of a set of UEs together simultaneously. Based on the VMIMO scheme, a novel 2D-DOA estimation algorithm in the scenario that uncorrelated signals and coherent signals coexist in the presence of unknown mutual coupling is proposed. The 2D-DOA of uncorrelated signals and coherent signals can be estimated by the DOA matrix method. The mutual coupling coefficients are estimated without the help of any calibration sources at known locations. Although the "blind angles" phenomenon may be happen with some particular angles. Fortunately, the lost angle can be found back in the estimation of coherent signals. Simulation results validate the effectiveness of the proposed method. The proposed algorithm can estimate 2D-DOA in parallel, which is suitable for practical application. Compared with the traditional sequential scheme, the VMIMO scheme can save more energy, which will have a prosperous application in 5G wireless communication systems.

Acknowledgments This work was supported in part by the Qing Lan Project, the National Science Foundation of China under Grant 61201410 and 61401147, the Natural Science Foundation of JiangSu Province of China,No.BK20140248, the Fundamental Research Funds for the Central Universities (Program No. HEUCF140803).This work has been partially supported by *Instituto de Telecomunicações*, Next Generation Networks and Applications Group (NetGNA), Covilhã Delegation, by Government of Russian Federation, Grant 074-U01, and by National Funding from the FCT - *Fundação para a Ciência e a Tecnologia* through the Pest-OE/EEI/LA0008/2013 Project.

Appendix

The Cramer–Rao lower bound (CRB) of 1D-DOA estimation in the presence of mutual coupling is given in [12,37]. In this Appendix, the CRB of joint 2D-DOA and mutual coupling estimation is derived. Consider the array output vector $\mathbf{x}(t)$

as a complex Gaussian vector with zero mean. Define $\mathbf{A} \triangleq [\mathbf{A}_c, \mathbf{A}_u]$, $\mathbf{E} \triangleq blkdiag\left[\mathbf{\Gamma}, \mathbf{I}_{K_u}\right]$, the covariance matrix of $\mathbf{x}(t)$ is expressed as

$$\mathbf{R}_x = E\left\{\mathbf{x}(t)\,\mathbf{x}(t)^H\right\} = \mathbf{CAER}_s\mathbf{E}^H\mathbf{A}^H\mathbf{C}^H \tag{64}$$

For L statistically independent observations of $\mathbf{x}(t)$, the logarithm of the likelihood function (the joint probability density function, PDF) can be written as [2,38]

$$\begin{aligned}\mathbf{\Theta} &= \ln\{f(\mathbf{x}(1), \mathbf{x}(2), \ldots, \mathbf{x}(L))\}\\ &= const - L\cdot\ln\{\det\{\mathbf{R}_x\}\}\\ &\quad -\sum_{t=1}^{L}\mathbf{x}(t)^H\mathbf{R}_x^{-1}\mathbf{x}(t)\\ &= const - L\cdot\ln\{\det\{\mathbf{R}_x\}\}\\ &\quad -L\cdot tr\left\{\mathbf{R}_x^{-1}\widehat{\mathbf{R}}_x\right\}\end{aligned} \tag{65}$$

where the estimate of auto-correlation covariance $\widehat{\mathbf{R}}_x$ is given by

$$\widehat{\mathbf{R}}_x = \frac{1}{L}\sum_{l=1}^{L}\mathbf{x}(l)\,\mathbf{x}(l)^H. \tag{66}$$

The unknown parameter vector of $\mathbf{R}_x$ is defined as

$$\begin{aligned}\boldsymbol{\eta} &= \left[\boldsymbol{\alpha}^T, \boldsymbol{\beta}^T, \boldsymbol{\mu}^T, \boldsymbol{\nu}^T, \boldsymbol{\kappa}^T, \boldsymbol{\varsigma}^T\right]^T\\ \boldsymbol{\alpha} &= [\alpha_{11}, \ldots, \alpha_{1L_1}, \ldots, \alpha_{P_1}, \ldots, \alpha_{PL_P},\\ &\quad \alpha_{K_c+1}, \ldots, \alpha_K]^T\\ \boldsymbol{\beta} &= [\beta_{11}, \ldots, \beta_{1L_1}, \ldots, \beta_{P_1}, \ldots, \beta_{PL_P},\\ &\quad \beta_{K_c+1}, \ldots, \beta_K]^T\end{aligned} \tag{67}$$

In order to obtain the unique CRB of $\boldsymbol{\rho}_k$, the fading coefficient of the signal in the pth group is normalized to unity. For the sake of simplify, α_{p1} is assumed to be the smallest DOA in the pth group in the following derivation. $\boldsymbol{\mu} = [\mu_{12}, \ldots, \mu_{1L_1}, \ldots, \mu_{P_2}, \ldots, \mu_{PL_P}]^T$ and $\boldsymbol{\nu} = [\nu_{12}, \ldots, \nu_{1L_1}, \ldots, \nu_{P_2}, \ldots, \nu_{PL_P}]^T$ are defined as the real part and $\boldsymbol{\varpi} = [\boldsymbol{\rho}_1(2:P_1)^T, \ldots, \boldsymbol{\rho}_D(2:P_D)^T]^T$ is defined as the imaginary part, respectively. $\boldsymbol{\kappa}$ and $\boldsymbol{\varsigma}$ are defined as the real part and imaginary part of $\mathbf{c}_1$, respectively. The kth element in a vector, for example, $\boldsymbol{\eta}$ is defined as η_k. Then the general expression of the (m,n)th element in Fisher information matrix (FIM) can be expressed as

$$\mathbf{F}_{\eta_m\eta_n} = -E\left\{\frac{\partial^2\Theta}{\partial\eta_m\partial\eta_n}\right\} \tag{68}$$

Based on the relationship

$$\frac{\partial\mathbf{R}_x^{-1}}{\partial\eta_m} = -\mathbf{R}_x^{-1}\frac{\partial\mathbf{R}_x}{\partial\eta_m}\mathbf{R}_x^{-1} \tag{69}$$

$$\frac{\partial\ln\{\det\{\mathbf{R}_x\}\}}{\partial\eta_m} = tr\left\{\mathbf{R}_x^{-1}\frac{\partial\mathbf{R}_x}{\partial\eta_m}\right\} \tag{70}$$

the first derivative of Θ is obtained

$$\begin{aligned}\frac{\partial\Theta}{\partial\eta_m} &= -Ltr\left\{\mathbf{R}_x^{-1}\frac{\partial\mathbf{R}_x}{\partial\eta_m}\right\}\\ &\quad + Ltr\left\{\mathbf{R}_x^{-1}\frac{\partial\mathbf{R}_x}{\partial\eta_m}\mathbf{R}_x^{-1}\widehat{\mathbf{R}}_x\right\}\\ &= Ltr\left\{\mathbf{R}_x^{-1}\frac{\partial\mathbf{R}_x}{\partial\eta_m}\left(\mathbf{R}_x^{-1}\widehat{\mathbf{R}}_x - \mathbf{I}\right)\right\}.\end{aligned} \tag{71}$$

The second derivative of Θ is given by

$$\begin{aligned}\frac{\partial\Theta}{\partial\eta_m\eta_n} &= Ltr\left\{\mathbf{R}_x^{-1}\frac{\partial\mathbf{R}_x}{\partial\eta_m}\left(\mathbf{R}_x^{-1}\widehat{\mathbf{R}}_x - \mathbf{I}\right)\right\}\\ &= Ltr\left\{\left(\partial\left(\mathbf{R}_x^{-1}\frac{\partial\mathbf{R}_x}{\partial\eta_m}\right)\Big/\partial\eta_n\right)\left(\mathbf{R}_x^{-1}\widehat{\mathbf{R}}_x - \mathbf{I}\right)\right\}\\ &\quad + Ltr\left\{\mathbf{R}_x^{-1}\frac{\partial\mathbf{R}_x}{\partial\eta_m}\frac{\partial\left(\mathbf{R}_x^{-1}\widehat{\mathbf{R}}_x - \mathbf{I}\right)}{\partial\eta_n}\right\}\\ &= Ltr\left\{\left(\partial\left(\mathbf{R}_x^{-1}\frac{\partial\mathbf{R}_x}{\partial\eta_m}\right)\Big/\partial\eta_n\right)\left(\mathbf{R}_x^{-1}\widehat{\mathbf{R}}_x - \mathbf{I}\right)\right\}\\ &\quad - Ltr\left\{\mathbf{R}_x^{-1}\frac{\partial\mathbf{R}_x}{\partial\eta_m}\left(\mathbf{R}_x^{-1}\frac{\partial\mathbf{R}_x}{\partial\eta_n}\mathbf{R}_x^{-1}\widehat{\mathbf{R}}_x\right)\right\}.\end{aligned} \tag{72}$$

Due to $E\left\{\widehat{\mathbf{R}}_x\right\} = \mathbf{R}_x$, the expectation of both sides of (70) is taken, we have

$$\mathbf{F}_{\eta_m\eta_n} = Ltr\left\{\mathbf{R}_x^{-1}\frac{\partial\mathbf{R}_x}{\partial\eta_m}\mathbf{R}_x^{-1}\frac{\partial\mathbf{R}_x}{\partial\eta_n}\right\}. \tag{73}$$

In the subsequent derivation process, the FIM expression of mixed signals is derived. The notation $\widetilde{\mathbf{R}}_{\eta_m}$ defines $\partial\mathbf{R}/\partial\eta_m$.

Derivatives with respect to DOA

Based on the expression of covariance matrix (64), the partial derivative of $\mathbf{R}_x$ with respect to the mth element α_m of $\boldsymbol{\alpha}$ can be written as

$$\begin{aligned}\frac{\partial\mathbf{R}_x}{\partial\alpha_m} &= \mathbf{C}\widetilde{\mathbf{A}}_{\alpha_m}\mathbf{ER}_s\mathbf{E}^H\mathbf{A}^H\mathbf{C}^H\\ &\quad + \mathbf{CAER}_s\mathbf{E}^H\widetilde{\mathbf{A}}_{\alpha_m}^H\mathbf{C}^H.\end{aligned} \tag{74}$$

Based on $tr\left\{\mathbf{R} + \mathbf{R}^H\right\} = 2\mathrm{Re}\{tr\{\mathbf{R}\}\}$, we have

$$\begin{aligned}\mathbf{F}_{\alpha_m\alpha_n} &= Ltr\left\{\mathbf{R}_x^{-1}\frac{\partial\mathbf{R}_x}{\partial\alpha_m}\mathbf{R}_x^{-1}\frac{\partial\mathbf{R}_x}{\partial\alpha_n}\right\}\\ &= Ltr\left\{\mathbf{R}_x^{-1}\left(\mathbf{C}\widetilde{\mathbf{A}}_{\alpha_m}\mathbf{ER}_s\mathbf{E}^H\mathbf{A}^H\mathbf{C}^H\right.\right.\\ &\quad \left.\left. + \mathbf{CAER}_s\mathbf{E}^H\widetilde{\mathbf{A}}_{\alpha_m}^H\mathbf{C}^H\right) \times \mathbf{R}_x^{-1}\right.\end{aligned}$$

$$
\begin{aligned}
&\left(\mathbf{C}\widetilde{\mathbf{A}}_{\alpha_n}\mathbf{E}\mathbf{R}_s\mathbf{E}^H\mathbf{A}^H\mathbf{C}^H\right.\\
&\left.+\mathbf{C}\mathbf{A}\mathbf{E}\mathbf{R}_s\mathbf{E}^H\widetilde{\mathbf{A}}_{\alpha_n}^H\mathbf{C}^H\right)\Big\}\\
&=2L\mathrm{Re}\left\{tr\left\{\mathbf{R}_x^{-1}C\widetilde{\mathbf{A}}_{\alpha_m}\mathbf{E}\mathbf{R}_s\mathbf{E}^H\mathbf{A}^H\right.\right.\\
&\times\mathbf{C}^H\mathbf{R}_x^{-1}\mathbf{C}\widetilde{\mathbf{A}}_{\alpha_n}\mathbf{E}\mathbf{R}_s\mathbf{E}^H\mathbf{A}^H\mathbf{C}^H\\
&+\mathbf{R}_x^{-1}\mathbf{C}\mathbf{A}\mathbf{E}\mathbf{R}_s\mathbf{E}^H\widetilde{\mathbf{A}}_{\alpha_m}^H\\
&\left.\left.\times\mathbf{C}^H\mathbf{R}_x^{-1}\mathbf{C}\widetilde{\mathbf{A}}_{\alpha_n}\mathbf{E}\mathbf{R}_s\mathbf{E}^H\mathbf{A}^H\mathbf{C}^H\right\}\right\}
\end{aligned}
\tag{75}
$$

Since only the mth column of $\widetilde{\mathbf{A}}_{\alpha_m}$ is nonzero, then $\widetilde{\mathbf{A}}_{\alpha_m}$ can be represented as $\widetilde{\mathbf{A}}_{\alpha_m}=\mathbf{A}_{\boldsymbol{\alpha}}\boldsymbol{\gamma}_K^m\left(\boldsymbol{\gamma}_K^m\right)^T$, where the mth column of the identity matrix is defined as $\boldsymbol{\gamma}_K^m$. $\mathbf{A}_{\boldsymbol{\alpha}}$ is the derivative matrix of the array manifold matrix, which is expressed as

$$
\begin{aligned}
\mathbf{A}_{\boldsymbol{\alpha}}=&\left[\frac{d\mathbf{a}\left(\alpha_{11}\right)}{d\alpha_{11}},\ldots,\frac{d\mathbf{a}\left(\alpha_{1P_1}\right)}{d\alpha_{1P_1}},\ldots,\frac{d\mathbf{a}\left(\alpha_{D1}\right)}{d\alpha_{D1}},\right.\\
&\left.\ldots,\frac{d\mathbf{a}\left(\alpha_{DP_D}\right)}{d\alpha_{DP_D}},\frac{d\mathbf{a}\left(\alpha_{K_c+1}\right)}{d\alpha_{K_c+1}},\ldots,\frac{d\mathbf{a}\left(\alpha_K\right)}{d\alpha_K}\right]^T
\end{aligned}
\tag{76}
$$

Then (73) can be written as

$$
\begin{aligned}
\mathbf{F}_{\alpha_m\alpha_n}=&2L\mathrm{Re}\{tr\left\{\mathbf{R}_x^{-1}\mathbf{C}\mathbf{A}_{\boldsymbol{\alpha}}\boldsymbol{\gamma}_K^m\left(\boldsymbol{\gamma}_K^m\right)^T\mathbf{E}\mathbf{R}_s\mathbf{E}^H\mathbf{A}^H\right.\\
&\times\mathbf{C}^H\mathbf{R}_x^{-1}\mathbf{C}\mathbf{A}_{\boldsymbol{\alpha}}\boldsymbol{\gamma}_K^n\left(\boldsymbol{\gamma}_K^n\right)^T\mathbf{E}\mathbf{R}_s\mathbf{E}^H\mathbf{A}^H\mathbf{C}^H\\
&+\mathbf{R}_x^{-1}\mathbf{C}\mathbf{A}\mathbf{E}\mathbf{R}_s\mathbf{E}^H\boldsymbol{\gamma}_K^m\left(\boldsymbol{\gamma}_K^m\right)^T\mathbf{A}_{\boldsymbol{\alpha}}^H\times\\
&\left.\mathbf{C}^H\mathbf{R}_x^{-1}\mathbf{C}\mathbf{A}_{\boldsymbol{\alpha}}\boldsymbol{\gamma}_K^n\left(\boldsymbol{\gamma}_K^n\right)^T\mathbf{E}\mathbf{R}_s\mathbf{E}^H\mathbf{A}^H\mathbf{C}^H\right\}\Big\}\\
=&2L\mathrm{Re}\left\{\left(\left(\boldsymbol{\gamma}_K^m\right)^T\mathbf{E}\mathbf{R}_s\mathbf{E}^H\mathbf{A}^H\mathbf{C}^H\mathbf{R}_x^{-1}\mathbf{C}\mathbf{A}_{\boldsymbol{\alpha}}\boldsymbol{\gamma}_K^n\right)\right.\\
&\times\left(\left(\boldsymbol{\gamma}_K^n\right)^T\mathbf{E}\mathbf{R}_s\mathbf{E}^H\mathbf{A}^H\mathbf{C}^H\mathbf{R}_x^{-1}\mathbf{C}\mathbf{A}_{\boldsymbol{\alpha}}\boldsymbol{\gamma}_K^m\right)\\
&+\left(\left(\boldsymbol{\gamma}_K^m\right)^T\mathbf{A}_{\boldsymbol{\alpha}}^H\mathbf{C}^H\mathbf{R}_x^{-1}\mathbf{C}\mathbf{A}_{\boldsymbol{\alpha}}\boldsymbol{\gamma}_K^n\right)\times\\
&\left.\left(\left(\boldsymbol{\gamma}_K^n\right)^T\mathbf{E}\mathbf{R}_s\mathbf{E}^H\mathbf{A}^H\mathbf{C}^H\mathbf{R}_x^{-1}\mathbf{C}\mathbf{A}\mathbf{E}\mathbf{R}_s\mathbf{E}^H\boldsymbol{\gamma}_K^m\right)\right\}
\end{aligned}
\tag{77}
$$

Then the FIM that corresponds to $\boldsymbol{\alpha}$ can be expressed as

$$
\begin{aligned}
\mathbf{F}_{\boldsymbol{\alpha}\boldsymbol{\alpha}}=&2L\mathrm{Re}\left\{\left(\mathbf{E}\mathbf{R}_s\mathbf{E}^H\mathbf{A}^H\mathbf{C}^H\mathbf{R}_x^{-1}\mathbf{C}\mathbf{A}_{\boldsymbol{\alpha}}\right)\right.\\
&\odot\left(\mathbf{E}\mathbf{R}_s\mathbf{E}^H\mathbf{A}^H\mathbf{C}^H\mathbf{R}_x^{-1}\mathbf{C}\mathbf{A}_{\boldsymbol{\alpha}}\right)^T\\
&+\left(\mathbf{A}_{\boldsymbol{\alpha}}^H\mathbf{C}^H\mathbf{R}_x^{-1}\mathbf{C}\mathbf{A}_{\boldsymbol{\alpha}}\right)\\
&\left.\odot\left(\mathbf{E}\mathbf{R}_s\mathbf{E}^H\mathbf{A}^H\mathbf{C}^H\mathbf{R}_x^{-1}\mathbf{C}\mathbf{A}\mathbf{E}\mathbf{R}_s\mathbf{E}^H\right)^T\right\}
\end{aligned}
\tag{78}
$$

where $\odot$ denotes the Hadamard product. Similarly, the FIM that corresponds to $\boldsymbol{\beta}$ can be expressed as

$$
\begin{aligned}
\mathbf{F}_{\boldsymbol{\beta}\boldsymbol{\beta}}=&2L\mathrm{Re}\left\{\left(\mathbf{E}\mathbf{R}_s\mathbf{E}^H\mathbf{A}^H\mathbf{C}^H\mathbf{R}_x^{-1}\mathbf{C}\mathbf{A}_{\boldsymbol{\beta}}\right)\right.\\
&\odot\left(\mathbf{E}\mathbf{R}_s\mathbf{E}^H\mathbf{A}^H\mathbf{C}^H\mathbf{R}_x^{-1}\mathbf{C}\mathbf{A}_{\boldsymbol{\beta}}\right)^T\\
&+\left(\mathbf{A}_{\boldsymbol{\beta}}^H\mathbf{C}^H\mathbf{R}_x^{-1}\mathbf{C}\mathbf{A}_{\boldsymbol{\beta}}\right)\\
&\left.\odot\left(\mathbf{E}\mathbf{R}_s\mathbf{E}^H\mathbf{A}^H\mathbf{C}^H\mathbf{R}_x^{-1}\mathbf{C}\mathbf{A}\mathbf{E}\mathbf{R}_s\mathbf{E}^H\right)^T\right\}
\end{aligned}
\tag{79}
$$

where

$$
\begin{aligned}
\mathbf{A}_{\boldsymbol{\alpha}}=&\left[\frac{d\mathbf{a}\left(\beta_{11}\right)}{d\beta_{11}},\ldots,\frac{d\mathbf{a}\left(\beta_{1P_1}\right)}{d\beta_{1P_1}},\ldots,\frac{d\mathbf{a}\left(\beta_{D1}\right)}{d\beta_{D1}},\right.\\
&\left.\ldots,\frac{d\mathbf{a}\left(\beta_{DP_D}\right)}{d\beta_{DP_D}},\frac{d\mathbf{a}\left(\beta_{K_c+1}\right)}{d\beta_{K_c+1}},\ldots,\frac{d\mathbf{a}\left(\beta_K\right)}{d\beta_K}\right]^T.
\end{aligned}
\tag{80}
$$

The FIM that corresponds to the cross terms between $\boldsymbol{\alpha}$ and $\boldsymbol{\beta}$ is

$$
\begin{aligned}
\mathbf{F}_{\boldsymbol{\alpha}\boldsymbol{\beta}}=&2L\mathrm{Re}\left\{\left(\mathbf{E}\mathbf{R}_s\mathbf{E}^H\mathbf{A}^H\mathbf{C}^H\mathbf{R}_x^{-1}\mathbf{C}\mathbf{A}_{\boldsymbol{\beta}}\right)\right.\\
&\odot\left(\mathbf{E}\mathbf{R}_s\mathbf{E}^H\mathbf{A}^H\mathbf{C}^H\mathbf{R}_x^{-1}\mathbf{C}\mathbf{A}_{\boldsymbol{\alpha}}\right)^T\\
&+\left(\mathbf{A}_{\boldsymbol{\alpha}}^H\mathbf{C}^H\mathbf{R}_x^{-1}\mathbf{C}\mathbf{A}_{\boldsymbol{\beta}}\right)\\
&\left.\odot\left(\mathbf{E}\mathbf{R}_s\mathbf{E}^H\mathbf{A}^H\mathbf{C}^H\mathbf{R}_x^{-1}\mathbf{C}\mathbf{A}\mathbf{E}\mathbf{R}_s\mathbf{E}^H\right)^T\right\}
\end{aligned}
\tag{81}
$$

Derivatives with respect to fading coefficients

$\overline{\mathbf{A}}_c=\left[\mathbf{A}_{c1}\left(1:N,2:L_1\right),\ldots,\mathbf{A}_{cD}\left(1:N,2:L_P\right)\right]$, and $\overline{\boldsymbol{\Gamma}}=blkdiag\left\{\boldsymbol{\rho}_1\left(2:L_1\right),\ldots,\boldsymbol{\rho}_D\left(2:L_P\right)\right\}$. The matrix $\boldsymbol{\Psi}_{\mathbf{r}}=blkdiag\left\{\mathbf{1}_{(L_1-1)\times1},\ldots,\mathbf{1}_{(L_P-1)\times1}\right\}$ and $\boldsymbol{\Psi}_{\mathbf{i}}=blkdiag\left\{\mathbf{j}_{(L_1-1)\times1},\ldots,\mathbf{j}_{(L_P-1)\times1}\right\}$, where all the elements of the vector $\mathbf{1}$ are equal to 1 and all the elements of the vector $\mathbf{j}$ are equal to the imaginary unit j. According to (73), the (r_m,r_n)th element of the FIM with respect to fading coefficients can be expressed as

$$
\begin{aligned}
\mathbf{F}_{\mu_m\mu_n}=&Ltr\left\{\mathbf{R}_x^{-1}\frac{\partial\mathbf{R}_x}{\partial\mu_m}\mathbf{R}_x^{-1}\frac{\partial\mathbf{R}_x}{\partial\mu_n}\right\}\\
=&Ltr\left\{\mathbf{R}_x^{-1}\left(\mathbf{C}\mathbf{A}\widetilde{\mathbf{E}}_{\mu_m}\mathbf{R}_s\mathbf{E}^H\mathbf{A}^H\mathbf{C}^H\right.\right.\\
&\left.+\mathbf{C}\mathbf{A}\mathbf{E}\mathbf{R}_s\mathbf{E}_{\mu_m}^H\mathbf{A}^H\mathbf{C}^H\right)\\
&\times\mathbf{R}_x^{-1}\left(\mathbf{C}\mathbf{A}\widetilde{\mathbf{E}}_{\mu_n}\mathbf{R}_s\mathbf{E}^H\mathbf{A}^H\mathbf{C}^H\right.\\
&\left.\left.+\mathbf{C}\mathbf{A}\mathbf{E}\mathbf{R}_s\mathbf{E}_{\mu_n}^H\mathbf{A}^H\mathbf{C}^H\right)\right\}\\
=&Ltr\left\{\mathbf{R}_x^{-1}\left(\mathbf{C}\overline{\mathbf{A}}_c\widetilde{\overline{\boldsymbol{\Gamma}}}_{\mu_m}\mathbf{R}_{cs}\boldsymbol{\Gamma}^H\mathbf{A}_c^H\mathbf{C}^H\right.\right.\\
&\left.+\mathbf{C}\mathbf{A}_c\boldsymbol{\Gamma}\mathbf{R}_{cs}\widetilde{\overline{\boldsymbol{\Gamma}}}_{\mu_m}^H\overline{\mathbf{A}}_c^H\mathbf{C}^H\right)\\
&\times\mathbf{R}_x^{-1}\left(\mathbf{C}\overline{\mathbf{A}}_c\widetilde{\overline{\boldsymbol{\Gamma}}}_{\mu_n}\mathbf{R}_{cs}\boldsymbol{\Gamma}^H\mathbf{A}_c^H\mathbf{C}^H\right.\\
&\left.\left.+\mathbf{C}\mathbf{A}_c\boldsymbol{\Gamma}\mathbf{R}_{cs}\widetilde{\overline{\boldsymbol{\Gamma}}}_{\mu_n}^H\overline{\mathbf{A}}_c^H\mathbf{C}^H\right)\right\}\\
=&2L\mathrm{Re}\left\{tr\left\{\mathbf{R}_x^{-1}\mathbf{C}\overline{\mathbf{A}}_c\widetilde{\overline{\boldsymbol{\Gamma}}}_{\mu_m}\mathbf{R}_{cs}\boldsymbol{\Gamma}^H\mathbf{A}_c^H\right.\right.
\end{aligned}
$$

$$\times \mathbf{C}^H\mathbf{R}_x^{-1}\mathbf{C}\overline{\mathbf{A}}_c\overline{\widetilde{\mathbf{\Gamma}}}_{\mu_n}\mathbf{R}_{cs}\mathbf{\Gamma}^H\mathbf{A}_c^H\mathbf{C}^H + \mathbf{R}_x^{-1}\mathbf{C}\mathbf{A}_c\mathbf{\Gamma}\mathbf{R}_{cs}\overline{\widetilde{\mathbf{\Gamma}}}^H_{\mu_m}\overline{\mathbf{A}}_c^H \mathbf{C}^H\mathbf{R}_x^{-1}\mathbf{C}\overline{\mathbf{A}}_c\overline{\widetilde{\mathbf{\Gamma}}}_{\mu_n}\mathbf{R}_{cs}\mathbf{\Gamma}^H\mathbf{A}_c^H\mathbf{C}^H\Big\}\Big\} \tag{82}$$

Based on $\overline{\mathbf{\Gamma}}_{\mu_m} = \boldsymbol{\gamma}^m_{K_c-P}\left(\boldsymbol{\gamma}^m_{K_c-P}\right)^T\mathbf{\Psi_r}$, the real part of fading coefficients of the FIM can be represented as

$$\begin{aligned} F_{\mu\mu} &= 2L\mathrm{Re}\Big\{\mathbf{R}_x^{-1}\mathbf{C}\overline{\mathbf{A}}_c\overline{\widetilde{\mathbf{\Gamma}}}_{\mu_m}\mathbf{R}_{cs}\mathbf{\Gamma}^H\mathbf{A}_c^H \times \mathbf{C}^H\mathbf{R}_x^{-1}\mathbf{C}\overline{\mathbf{A}}_c\overline{\widetilde{\mathbf{\Gamma}}}_{\mu_n}\mathbf{R}_{cs}\mathbf{\Gamma}^H\mathbf{A}_c^H\mathbf{C}^H + \mathbf{R}_x^{-1}\mathbf{C}\mathbf{A}_c\mathbf{\Gamma}\mathbf{R}_{cs}\overline{\widetilde{\mathbf{\Gamma}}}^H_{\mu_m}\overline{\mathbf{A}}_c^H \times \mathbf{C}^H\mathbf{R}_x^{-1}\mathbf{C}\overline{\mathbf{A}}_c\overline{\widetilde{\mathbf{\Gamma}}}_{\mu_n}\mathbf{R}_{cs}\mathbf{\Gamma}^H\mathbf{A}_c^H\mathbf{C}^H\Big\} \\ &= 2L\mathrm{Re}\Big\{\left(\mathbf{\Psi_r}\mathbf{R}_{cs}\mathbf{\Gamma}^H\mathbf{A}_c^H\mathbf{C}^H\mathbf{R}_x^{-1}\mathbf{C}\overline{\mathbf{A}}_c\right) \odot \left(\mathbf{\Psi_r}\mathbf{R}_{cs}\mathbf{\Gamma}^H\mathbf{A}_c^H\mathbf{C}^H\mathbf{R}_x^{-1}\mathbf{C}\overline{\mathbf{A}}_c\right)^T + \left(\overline{\mathbf{A}}_c^H\mathbf{C}^H\mathbf{R}_x^{-1}\mathbf{C}\overline{\mathbf{A}}_c\right) \odot \left(\mathbf{\Psi_r}\mathbf{R}_{cs}\mathbf{\Gamma}^H\mathbf{A}_c^H\mathbf{C}^H\mathbf{R}_x^{-1}\mathbf{C}\mathbf{A}_c\mathbf{\Gamma}\mathbf{R}_{cs}\mathbf{\Psi}_\mathbf{r}^H\right)^T\Big\} \end{aligned} \tag{83}$$

Based on $\overline{\mathbf{\Gamma}}_{\nu_m} = \boldsymbol{\gamma}^m_{K_c-P}\left(\boldsymbol{\gamma}^m_{K_c-P}\right)^T\mathbf{\Psi_i}$, the imaginary part of fading coefficients of the FIM can be represented as

$$\begin{aligned} \mathbf{F}_{\nu\nu} &= 2L\mathrm{Re}\Big\{\left(\mathbf{\Psi_i}\mathbf{R}_{cs}\mathbf{\Gamma}^H\mathbf{A}_c^H\mathbf{C}^H\mathbf{R}_x^{-1}\mathbf{C}\overline{\mathbf{A}}_c\right) \odot \left(\mathbf{\Psi_i}\mathbf{R}_{cs}\mathbf{\Gamma}^H\mathbf{A}_c^H\mathbf{C}^H\mathbf{R}_x^{-1}\mathbf{C}\overline{\mathbf{A}}_c\right)^T + \left(\overline{\mathbf{A}}_c^H\mathbf{C}^H\mathbf{R}_x^{-1}\mathbf{C}\overline{\mathbf{A}}_c\right) \odot \left(\mathbf{\Psi_i}\mathbf{R}_{cs}\mathbf{\Gamma}^H\mathbf{A}_c^H\mathbf{C}^H\mathbf{R}_x^{-1}\mathbf{C}\mathbf{A}_c\mathbf{\Gamma}\mathbf{R}_{cs}\mathbf{\Psi}_\mathbf{i}^H\right)^T\Big\} \end{aligned} \tag{84}$$

The FIM that corresponds to the cross terms between $\boldsymbol{\mu}$ and $\boldsymbol{\nu}$ is

$$\begin{aligned} \mathbf{F}_{\mu\nu} &= 2L\mathrm{Re}\Big\{\left(\mathbf{\Psi_r}\mathbf{R}_{cs}\mathbf{\Gamma}^H\mathbf{A}_c^H\mathbf{C}^H\mathbf{R}_x^{-1}\mathbf{C}\overline{\mathbf{A}}_c\right) \odot \left(\mathbf{\Psi_i}\mathbf{R}_{cs}\mathbf{\Gamma}^H\mathbf{A}_c^H\mathbf{C}^H\mathbf{R}_x^{-1}\mathbf{C}\overline{\mathbf{A}}_c\right)^T + \left(\overline{\mathbf{A}}_c^H\mathbf{C}^H\mathbf{R}_x^{-1}\mathbf{C}\overline{\mathbf{A}}_c\right) \odot \left(\mathbf{\Psi_i}\mathbf{R}_{cs}\mathbf{\Gamma}^H\mathbf{A}_c^H\mathbf{C}^H\mathbf{R}_x^{-1}\mathbf{C}\mathbf{A}_c\mathbf{\Gamma}\mathbf{R}_{cs}\mathbf{\Psi}_\mathbf{r}^H\right)^T\Big\} \end{aligned} \tag{85}$$

Derivatives with respect to mutual coupling coefficients

Based on (73), the mth and nth element of $\mathbf{F}_{\kappa\kappa}$, $\mathbf{F}_{\varsigma\varsigma}$ and $\mathbf{F}_{\kappa\varsigma}$ can be given respectively as follows

$$\begin{aligned} \mathbf{F}_{\kappa_m\kappa_n} &= 2L\mathrm{Re}\Big\{tr\Big\{\mathbf{R}_x^{-1}\widetilde{\mathbf{C}}_{\kappa_m}\mathbf{A}\mathbf{E}\mathbf{R}_s\mathbf{E}^H\mathbf{A}^H \times \mathbf{C}^H\mathbf{R}_x^{-1}\widetilde{\mathbf{C}}_{\kappa_n}\mathbf{A}\mathbf{E}\mathbf{R}_s\mathbf{E}^H\mathbf{A}^H\mathbf{C}^H + \mathbf{R}_x^{-1}\widetilde{\mathbf{C}}_{\kappa_m}\mathbf{A}\mathbf{E}\mathbf{R}_s\mathbf{E}^H\mathbf{A}^H \times \mathbf{C}^H\mathbf{R}_x^{-1}\mathbf{C}\mathbf{A}\mathbf{E}\mathbf{R}_s\mathbf{E}^H\mathbf{A}^H\mathbf{C}_{\kappa_n}^H\Big\}\Big\} \end{aligned} \tag{86}$$

$$\begin{aligned} \mathbf{F}_{\varsigma_m\varsigma_n} &= 2L\mathrm{Re}\Big\{tr\Big\{\mathbf{R}_x^{-1}\widetilde{\mathbf{C}}_{\varsigma_m}\mathbf{A}\mathbf{E}\mathbf{R}_s\mathbf{E}^H\mathbf{A}^H \times \mathbf{C}^H\mathbf{R}_x^{-1}\widetilde{\mathbf{C}}_{\varsigma_n}\mathbf{A}\mathbf{E}\mathbf{R}_s\mathbf{E}^H\mathbf{A}^H\mathbf{C}^H + \mathbf{R}_x^{-1}\widetilde{\mathbf{C}}_{\varsigma_m}\mathbf{A}\mathbf{E}\mathbf{R}_s\mathbf{E}^H\mathbf{A}^H \times \mathbf{C}^H\mathbf{R}_x^{-1}\mathbf{C}\mathbf{A}\mathbf{E}\mathbf{R}_s\mathbf{E}^H\mathbf{A}^H\mathbf{C}_{\varsigma_n}^H\Big\}\Big\} \end{aligned} \tag{87}$$

$$\begin{aligned} \mathbf{F}_{\kappa_m\varsigma_n} &= 2L\mathrm{Re}\Big\{tr\Big\{\mathbf{R}_x^{-1}\widetilde{\mathbf{C}}_{\kappa_m}\mathbf{A}\mathbf{E}\mathbf{R}_s\mathbf{E}^H\mathbf{A}^H \times \mathbf{C}^H\mathbf{R}_x^{-1}\widetilde{\mathbf{C}}_{\varsigma_n}\mathbf{A}\mathbf{E}\mathbf{R}_s\mathbf{E}^H\mathbf{A}^H\mathbf{C}^H + \mathbf{R}_x^{-1}\widetilde{\mathbf{C}}_{\kappa_m}\mathbf{A}\mathbf{E}\mathbf{R}_s\mathbf{E}^H\mathbf{A}^H \times \mathbf{C}^H\mathbf{R}_x^{-1}\mathbf{C}\mathbf{A}\mathbf{E}\mathbf{R}_s\mathbf{E}^H\mathbf{A}^H\mathbf{C}_{\varsigma_n}^H\Big\}\Big\} \end{aligned} \tag{88}$$

where

$$\widetilde{\mathbf{C}}_{\kappa_m} = toeplitz\left\{\left[0, \left(\boldsymbol{\gamma}^m_{M_0}\right)^T, \mathbf{0}_{1,(M-M_0-1)}\right]\right\}, \quad m = 1, \ldots, M_0. \tag{89}$$

$toeplitz\{\mathbf{z}\}$ stands for the symmetric Toeplitz matrix constructed by the vector $\mathbf{z}$.

DOA-fading coefficients cross terms

$$\begin{aligned} \mathbf{F}_{\alpha\mu} &= 2L\mathrm{Re}\Big\{\left(\mathbf{E}\mathbf{R}_s\mathbf{E}^H\mathbf{A}^H\mathbf{C}^H\mathbf{R}_x^{-1}\mathbf{C}\overline{\mathbf{A}}_c\right) \odot \left(\mathbf{\Psi_r}\mathbf{R}_{cs}\mathbf{\Gamma}^H\mathbf{A}_c^H\mathbf{C}^H\mathbf{R}_x^{-1}\mathbf{C}\mathbf{A}_{\boldsymbol{\alpha}}\right)^T + \left(\mathbf{A}_{\boldsymbol{\alpha}}^H\mathbf{C}^H\mathbf{R}_x^{-1}\mathbf{C}\overline{\mathbf{A}}_c\right) \odot \left(\mathbf{\Psi_r}\mathbf{R}_{cs}\mathbf{\Gamma}^H\mathbf{A}_c^H\mathbf{C}^H\mathbf{R}_x^{-1}\mathbf{C}\mathbf{A}\mathbf{E}\mathbf{R}_s\mathbf{E}^H\right)^T\Big\} \end{aligned} \tag{90}$$

$$\begin{aligned} \mathbf{F}_{\alpha\nu} &= 2L\mathrm{Re}\Big\{\left(\mathbf{E}\mathbf{R}_s\mathbf{E}^H\mathbf{A}^H\mathbf{C}^H\mathbf{R}_x^{-1}\mathbf{C}\overline{\mathbf{A}}_c\right) \odot \left(\mathbf{\Psi_i}\mathbf{R}_{cs}\mathbf{\Gamma}^H\mathbf{A}_c^H\mathbf{C}^H\mathbf{R}_x^{-1}\mathbf{C}\mathbf{A}_{\boldsymbol{\alpha}}\right)^T + \left(\mathbf{A}_{\boldsymbol{\alpha}}^H\mathbf{C}^H\mathbf{R}_x^{-1}\mathbf{C}\overline{\mathbf{A}}_c\right) \odot \left(\mathbf{\Psi_i}\mathbf{R}_{cs}\mathbf{\Gamma}^H\mathbf{A}_c^H\mathbf{C}^H\mathbf{R}_x^{-1}\mathbf{C}\mathbf{A}\mathbf{E}\mathbf{R}_s\mathbf{E}^H\right)^T\Big\} \end{aligned} \tag{91}$$

$$\begin{aligned} \mathbf{F}_{\beta\mu} &= 2L\mathrm{Re}\Big\{\left(\mathbf{E}\mathbf{R}_s\mathbf{E}^H\mathbf{A}^H\mathbf{C}^H\mathbf{R}_x^{-1}\mathbf{C}\overline{\mathbf{A}}_c\right) \odot \left(\mathbf{\Psi_r}\mathbf{R}_{cs}\mathbf{\Gamma}^H\mathbf{A}_c^H\mathbf{C}^H\mathbf{R}_x^{-1}\mathbf{C}\mathbf{A}_{\boldsymbol{\beta}}\right)^T + \left(\mathbf{A}_{\boldsymbol{\beta}}^H\mathbf{C}^H\mathbf{R}_x^{-1}\mathbf{C}\overline{\mathbf{A}}_c\right) \odot \left(\mathbf{\Psi_r}\mathbf{R}_{cs}\mathbf{\Gamma}^H\mathbf{A}_c^H\mathbf{C}^H\mathbf{R}_x^{-1}\mathbf{C}\mathbf{A}\mathbf{E}\mathbf{R}_s\mathbf{E}^H\right)^T\Big\} \end{aligned} \tag{92}$$

$$\begin{aligned} \mathbf{F}_{\beta\nu} &= 2L\mathrm{Re}\Big\{\left(\mathbf{E}\mathbf{R}_s\mathbf{E}^H\mathbf{A}^H\mathbf{C}^H\mathbf{R}_x^{-1}\mathbf{C}\overline{\mathbf{A}}_c\right) \odot \left(\mathbf{\Psi_i}\mathbf{R}_{cs}\mathbf{\Gamma}^H\mathbf{A}_c^H\mathbf{C}^H\mathbf{R}_x^{-1}\mathbf{C}\mathbf{A}_{\boldsymbol{\beta}}\right)^T + \left(\mathbf{A}_{\boldsymbol{\beta}}^H\mathbf{C}^H\mathbf{R}_x^{-1}\mathbf{C}\overline{\mathbf{A}}_c\right)\end{aligned}$$

$$\odot \left(\boldsymbol{\Psi}_{\mathbf{i}}\mathbf{R}_{cs}\boldsymbol{\Gamma}^H\mathbf{A}_c^H\mathbf{C}^H\mathbf{R}_x^{-1}\mathbf{CAER}_s\mathbf{E}^H\right)^T\Big\} \quad (93)$$

DOA-mutual coupling coefficients cross terms

$$\begin{aligned}\mathbf{F}_{\boldsymbol{\alpha}\kappa_n} = 2L\mathrm{Re}\Big\{&diag\left(\mathbf{ER}_s\mathbf{E}^H\mathbf{A}^H\mathbf{C}^H\mathbf{R}_x^{-1}\widetilde{\mathbf{C}}_{\kappa_n}\right.\\ &\times\left.\mathbf{AER}_s\mathbf{E}^H\mathbf{A}^H\mathbf{C}^H\mathbf{R}_x^{-1}\mathbf{CA}_{\boldsymbol{\alpha}}\right)\\ &+diag\left(\mathbf{ER}_s\mathbf{E}^H\mathbf{A}^H\mathbf{C}^H\mathbf{R}_x^{-1}\mathbf{C}\right.\\ &\times\left.\mathbf{AER}_s\mathbf{E}^H\mathbf{A}^H\widetilde{\mathbf{C}}_{\kappa_n}^H\mathbf{R}_x^{-1}\mathbf{CA}_{\boldsymbol{\alpha}}\right)\Big\}\end{aligned} \quad (94)$$

$$\begin{aligned}\mathbf{F}_{\boldsymbol{\alpha}\varsigma_n} = 2L\mathrm{Re}\Big\{&diag\left(\mathbf{ER}_s\mathbf{E}^H\mathbf{A}^H\mathbf{C}^H\mathbf{R}_x^{-1}\widetilde{\mathbf{C}}_{\varsigma_n}\right.\\ &\times\left.\mathbf{AER}_s\mathbf{E}^H\mathbf{A}^H\mathbf{C}^H\mathbf{R}_x^{-1}\mathbf{CA}_{\boldsymbol{\alpha}}\right)\\ &+diag\left(\mathbf{ER}_s\mathbf{E}^H\mathbf{A}^H\mathbf{C}^H\mathbf{R}_x^{-1}\mathbf{C}\right.\\ &\times\left.\mathbf{AER}_s\mathbf{E}^H\mathbf{A}^H\widetilde{\mathbf{C}}_{\varsigma_n}^H\mathbf{R}_x^{-1}\mathbf{CA}_{\boldsymbol{\alpha}}\right)\Big\}\end{aligned} \quad (95)$$

$$\begin{aligned}\mathbf{F}_{\boldsymbol{\beta}\kappa_n} = 2L\mathrm{Re}\{&diag\left(\mathbf{ER}_s\mathbf{E}^H\mathbf{A}^H\mathbf{C}^H\mathbf{R}_x^{-1}\widetilde{\mathbf{C}}_{\kappa_n}\right.\\ &\times\left.\mathbf{AER}_s\mathbf{E}^H\mathbf{A}^H\mathbf{C}^H\mathbf{R}_x^{-1}\mathbf{CA}_{\boldsymbol{\beta}}\right)\\ &+diag\left(\mathbf{ER}_s\mathbf{E}^H\mathbf{A}^H\mathbf{C}^H\mathbf{R}_x^{-1}\mathbf{C}\times\right.\\ &\left.\mathbf{AER}_s\mathbf{E}^H\mathbf{A}^H\widetilde{\mathbf{C}}_{\kappa_n}^H\mathbf{R}_x^{-1}\mathbf{CA}_{\boldsymbol{\beta}}\right)\Big\}\end{aligned} \quad (96)$$

$$\begin{aligned}\mathbf{F}_{\boldsymbol{\beta}\varsigma_n} = 2L\mathrm{Re}\{&diag\left(\mathbf{ER}_s\mathbf{E}^H\mathbf{A}^H\mathbf{C}^H\mathbf{R}_x^{-1}\widetilde{\mathbf{C}}_{\varsigma_n}\right.\\ &\times\left.\mathbf{AER}_s\mathbf{E}^H\mathbf{A}^H\mathbf{C}^H\mathbf{R}_x^{-1}\mathbf{CA}_{\boldsymbol{\beta}}\right)\\ &+diag\left(\mathbf{ER}_s\mathbf{E}^H\mathbf{A}^H\mathbf{C}^H\mathbf{R}_x^{-1}\mathbf{C}\right.\\ &\times\left.\mathbf{AER}_s\mathbf{E}^H\mathbf{A}^H\widetilde{\mathbf{C}}_{\varsigma_n}^H\mathbf{R}_x^{-1}\mathbf{CA}_{\boldsymbol{\beta}}\right)\Big\}\end{aligned} \quad (97)$$

where $diag\,(\mathbf{A})$ is a column vector constructed by the main diagonal elements of matrix $\mathbf{A}$.

Fading coefficients-mutual coupling coefficients cross terms

$$\begin{aligned}\mathbf{F}_{\boldsymbol{\mu}\kappa_n} = 2L\mathrm{Re}\{&diag\left(\boldsymbol{\Psi}_{\mathbf{r}}\mathbf{R}_{cs}\boldsymbol{\Gamma}^H\mathbf{A}_c^H\mathbf{C}^H\mathbf{R}_x^{-1}\right.\\ &\times\left.\widetilde{\mathbf{C}}_{\kappa_n}\mathbf{AER}_s\mathbf{E}^H\mathbf{A}^H\mathbf{C}^H\mathbf{R}_x^{-1}\mathbf{C}\overline{\mathbf{A}}_c\right)\\ &+diag\left(\boldsymbol{\Psi}_{\mathbf{r}}\mathbf{R}_{cs}\boldsymbol{\Gamma}^H\mathbf{A}_c^H\mathbf{C}^H\mathbf{R}_x^{-1}\mathbf{C}\right.\\ &\times\left.\mathbf{AER}_s\mathbf{E}^H\mathbf{A}^H\widetilde{\mathbf{C}}_{\kappa_n}^H\mathbf{R}_x^{-1}\mathbf{C}\overline{\mathbf{A}}_c\right)\Big\}\end{aligned} \quad (98)$$

$$\begin{aligned}\mathbf{F}_{\boldsymbol{\mu}\varsigma_n} = 2L\mathrm{Re}\{&diag\left(\boldsymbol{\Psi}_{\mathbf{r}}\mathbf{R}_{cs}\boldsymbol{\Gamma}^H\mathbf{A}_c^H\mathbf{C}^H\mathbf{R}_x^{-1}\right.\\ &\times\left.\widetilde{\mathbf{C}}_{\varsigma_n}\mathbf{AER}_s\mathbf{E}^H\mathbf{A}^H\mathbf{C}^H\mathbf{R}_x^{-1}\mathbf{C}\overline{\mathbf{A}}_c\right)\\ &+diag\left(\boldsymbol{\Psi}_{\mathbf{r}}\mathbf{R}_{cs}\boldsymbol{\Gamma}^H\mathbf{A}_c^H\mathbf{C}^H\mathbf{R}_x^{-1}\mathbf{C}\right.\\ &\times\left.\mathbf{AER}_s\mathbf{E}^H\mathbf{A}^H\widetilde{\mathbf{C}}_{\varsigma_n}^H\mathbf{R}_x^{-1}\mathbf{C}\overline{\mathbf{A}}_c\right)\Big\}\end{aligned} \quad (99)$$

$$\begin{aligned}F_{\nu\kappa_n} = 2L\mathrm{Re}\{&diag\left(\boldsymbol{\Psi}_{\mathbf{i}}\mathbf{R}_{cs}\boldsymbol{\Gamma}^H\mathbf{A}_c^H\mathbf{C}^H\mathbf{R}_x^{-1}\right.\\ &\times\left.\widetilde{\mathbf{C}}_{\kappa_n}\mathbf{AER}_s\mathbf{E}^H\mathbf{A}^H\mathbf{C}^H\mathbf{R}_x^{-1}\mathbf{C}\overline{\mathbf{A}}_c\right)\\ &+diag\left(\boldsymbol{\Psi}_{\mathbf{i}}\mathbf{R}_{cs}\boldsymbol{\Gamma}^H\mathbf{A}_c^H\mathbf{C}^H\mathbf{R}_x^{-1}\right.\\ &\times\left.\mathbf{CAER}_s\mathbf{E}^H\mathbf{A}^H\widetilde{\mathbf{C}}_{\kappa_n}^H\mathbf{R}_x^{-1}\mathbf{C}\overline{\mathbf{A}}_c\right)\Big\}\end{aligned} \quad (100)$$

$$\begin{aligned}\mathbf{F}_{\nu\varsigma_n} = 2L\mathrm{Re}\{&diag\left(\boldsymbol{\Psi}_{\mathbf{i}}\mathbf{R}_{cs}\boldsymbol{\Gamma}^H\mathbf{A}_c^H\mathbf{C}^H\mathbf{R}_x^{-1}\right.\\ &\times\left.\widetilde{\mathbf{C}}_{\varsigma_n}\mathbf{AER}_s\mathbf{E}^H\mathbf{A}^H\mathbf{C}^H\mathbf{R}_x^{-1}\mathbf{C}\overline{\mathbf{A}}_c\right.\\ &+diag\left(\boldsymbol{\Psi}_{\mathbf{i}}\mathbf{R}_{cs}\boldsymbol{\Gamma}^H\mathbf{A}_c^H\mathbf{C}^H\mathbf{R}_x^{-1}\mathbf{C}\right.\\ &\times\left.\mathbf{AER}_s\mathbf{E}^H\mathbf{A}^H\widetilde{\mathbf{C}}_{\varsigma_n}^H\mathbf{R}_x^{-1}\mathbf{C}\overline{\mathbf{A}}_c\right)\Big\}\end{aligned} \quad (101)$$

Based on the above formulations, the whole FIM can be expressed as

$$\mathbf{F}_{\eta\eta} = \begin{bmatrix}\mathbf{F}_{\alpha\alpha} & \mathbf{F}_{\alpha\beta} & \mathbf{F}_{\alpha\mu} & \mathbf{F}_{\alpha\nu} & \mathbf{F}_{\alpha\kappa} & \mathbf{F}_{\alpha\varsigma}\\ \mathbf{F}_{\alpha\beta}^T & \mathbf{F}_{\beta\beta} & \mathbf{F}_{\beta\mu} & \mathbf{F}_{\beta\nu} & \mathbf{F}_{\beta\kappa} & \mathbf{F}_{\beta\varsigma}\\ \mathbf{F}_{\alpha\mu}^T & \mathbf{F}_{\beta\mu}^T & \mathbf{F}_{\mu\mu} & \mathbf{F}_{\mu\nu} & \mathbf{F}_{\mu\kappa} & \mathbf{F}_{\mu\varsigma}\\ \mathbf{F}_{\alpha\nu}^T & \mathbf{F}_{\beta\nu}^T & \mathbf{F}_{\mu\nu}^T & \mathbf{F}_{\nu\nu} & \mathbf{F}_{\nu\kappa} & \mathbf{F}_{\nu\varsigma}\\ \mathbf{F}_{\alpha\kappa}^T & \mathbf{F}_{\beta\kappa}^T & \mathbf{F}_{\mu\kappa}^T & \mathbf{F}_{\nu\kappa}^T & \mathbf{F}_{\kappa\kappa} & \mathbf{F}_{\kappa\varsigma}\\ \mathbf{F}_{\alpha\varsigma}^T & \mathbf{F}_{\beta\varsigma}^T & \mathbf{F}_{\mu\varsigma}^T & \mathbf{F}_{\nu\varsigma}^T & \mathbf{F}_{\kappa\varsigma}^T & \mathbf{F}_{\varsigma\varsigma}\end{bmatrix} \quad (102)$$

Define $\mathbf{H} = \mathbf{F}_{\eta\eta}^{-1}$, the CRBs of coherent signals, uncorrelated signals and mutual coupling coefficients can be given, respectively, as

$$CRB_{\Omega_c} = \sqrt{\frac{1}{2K_c}\left(\sum_{k=1}^{K_c}\mathbf{H}_{kk} + \sum_{k=K+1}^{K+K_c}\mathbf{H}_{kk}\right)} \quad (103)$$

$$CRB_{\Omega_u} = \sqrt{\frac{1}{2K_c}\left(\sum_{k=K_c+1}^{K}\mathbf{H}_{kk} + \sum_{k=K+K_c+1}^{2K}\mathbf{H}_{kk}\right)} \quad (104)$$

$$CRB_c = \sqrt{\frac{1}{\|\mathbf{c}_1\|}\left(\sum_{k=2(K+K_c-P)}^{2(K+K_c-P+M_0)}\mathbf{H}_{kk}\right)} \quad (105)$$

References

1. Aruna, T., & Suganthi, M. (2012). Variable power adaptive MIMO OFDM system under imperfect CSI for mobile ad hoc networks. *Telecommunication Systems*, *50*(1), 47–53.
2. Bao, Q., Ko, C. C., & Zhi, W. (2005). DOA estimation under unknown mutual coupling and multipath. *IEEE Transactions on Aerospace and Electronic Systems*, *41*(2), 565–573.
3. Cadzow, J. A., Kim, Y. S., Shiue, D., Sun, Y., & Xu, G. (1987). Resolution of coherent signals using a linear array. In *IEEE International Conference on Acoustics, Speech, and Signal Processing* (pp. 1597–1600).
4. Cadzow, J., Kim, Y., & Shiue, D. (1989). General direction-of - arrival estimation: A signal subspace approach. *IEEE Transactions on Aerospace and Electronic Systems*, *25*(1), 31–47.

5. Chen, H., Pan, Z., Tian, L., Shi, J., Yang, G., & Suzuki, M. (2013). A novel AWSF algorithm for DOA estimation in virtual MIMO systems. *IEEE Journal on Selected Areas in Communications*, *31*(10), 1994–2003.
6. Chen, Z., Yuan, J., & Vucetic, B. (2005). Analysis of transmit antenna selection/maximal-ratio combining in Rayleigh fading channels. *IEEE Transactions on Vehicular Technology*, *54*(4), 1312–1321.
7. Chung, J., Yun, Y., & Choi, S. (2013). Experiments on MIMO-OFDM system combined with adaptive beamforming based on IEEE 802.16 e WMAN standard. *Telecommunication Systems*, *52*(4), 1931–1944.
8. Dai, J., Xu, W., & Zhao, D. (2012). Real-valued DOA estimation for uniform linear array with unknown mutual coupling. *Signal Processing*, *92*(9), 2056–2065.
9. Dai, J., & Ye, Z. (2011). Spatial moothing for direction of arrival estimation of coherent signals in the presence of unknown mutual coupling. *IET Signal Processing*, *5*(4), 418–425.
10. Di, A., & Tian, L. (1984). Matrix decomposition and multiple source location. In *IEEE International Conference on Acoustics, Speech, and Signal Processing* (pp. 722–725).
11. Di, A. (1985). Multiple source location: A matrix decomposition approach. *IEEE Transactions on Acoustics, Speech and Signal Processing*, *33*(5), 1086–1091.
12. Friedlander, B., & Weiss, A. J. (1991). Direction finding in the presence of mutual coupling. *IEEE Transactions on Antennas and Propagation*, *39*(3), 273–284.
13. Gan, L., & Luo, X. (2013). Direction-of-arrival estimation for uncorrelated and coherent signals in the presence of multipath propagation. *IET Microwaves, Antennas & Propagation*, *7*(9), 746–753.
14. Han, G., Xu, H., Duong, T. Q., Jiang, J., & Hara, T. (2013). Localization algorithms of wireless sensor networks: A survey. *Telecommunication Systems*, *52*(4), 2419–2436.
15. He, J., & Liu, Z. (2009). Extended aperture 2-D direction finding with a two-parallel-shape-array using propagator method. *IEEE Antennas and Wireless Propagation Letters*, *8*, 323–327.
16. Jiang, J., Han, G., Zhu, C., Dong, Y., & Zhang, N. (2011). Secure localization in wireless sensor networks: A survey. *Journal of Communications*, *6*(6), 460–470.
17. Karimi, O. B., Toutounchian, M. A., Liu, J., & Wang, C. (2013). Lightweight user grouping with flexible degrees of freedom in virtual MIMO. *IEEE Journal on Selected Areas in Communications*, *31*(10), 2004–2012.
18. Kuchar, A., Tangemann, M., & Bonek, E. (2002). A real-time DOA-based smart antenna processor. *IEEE Transactions on Vehicular Technology*, *51*(6), 1279–1293.
19. Li, J., Zhang, X., & Chen, H. (2012). Improved two-dimensional DOA estimation algorithm for two-parallel uniform linear arrays using propagator method. *Signal Processing*, *92*(12), 3032–3038.
20. Li, P., Xu, J., & Yu, B. (1997). An efficient method in array processing for eliminating the signal cancellation phenomena of the differencing method. *Signal Processing*, *56*(3), 305–312.
21. Liu, F., Wang, J., Sun, C., & Du, R. (2012). Spatial differencing method for DOA estimation under the coexistence of both uncorrelated and coherent signals. *IEEE Transactions on Antennas and Propagation*, *60*(4), 2052–2062.
22. Liu, Z., Huang, Z., Wang, F., & Zhou, Y. (2009). DOA estimation with uniform linear arrays in the presence of mutual coupling via blind calibration. *Signal Processing*, *89*(7), 1446–1456.
23. Mohammadi, A., & Ghannouchi, F. M. (2011). Single RF front-end MIMO transceivers. *IEEE Communications Magazine*, *49*(12), 104–109.
24. Ntontin, K., Di Renzo, M., Perez-Neira, A., & Verikoukis, C. (2013). A low-complexity method for antenna selection in spatial modulation systems. *IEEE Communications Letters*, *17*(12), 2312–2315.
25. Qi, C., Wang, Y., Zhang, Y., & Han, Y. (2005). Spatial difference smoothing for DOA estimation of coherent signals. *IEEE Signal Processing Letters*, *12*(11), 800–802.
26. Roy, R., & Kailath, T. (1989). ESPRIT-estimation of signal parameters via rotational invariance techniques. *IEEE Transactions on Acoustics, Speech and Signal Processing*, *37*(7), 984–995.
27. Schmidt, R. O. (1986). Multiple emitter location and signal parameter estimation. *IEEE Transactions on Antennas and Propagation*, *34*(3), 276–280.
28. Swindlehurst, A. L., & Kailath, T. (1992). A performance analysis of subspace-based methods in the presence of model errors. I. The MUSIC algorithm. *IEEE Transactions on Signal Processing*, *40*(7), 1758–1774.
29. Tang, L., Chen, Q., Wang, G., Zeng, X., & Wang, H. (2013). Opportunistic power allocation strategies and fair subcarrier allocation in OFDM-based cognitive radio networks. *Telecommunication Systems*, *52*(4), 2071–2082.
30. Tao, H., Xin, J., Wang, J., Zheng, N., & Sano, A. (2013). Two-dimensional direction of arrival estimation method for a mixture of noncoherent and coherent narrowband signals. In *2013 IEEE 14th Workshop on Signal Processing Advances in Wireless Communications* (pp. 440–444).
31. Wang, H., & Liu, K. R. (1998). 2-D spatial smoothing for multipath coherent signal separation. *IEEE Transactions on Aerospace and Electronic Systems*, *34*(2), 391–405.
32. Wen, H., Gong, G., Lv, S. C., & Ho, P. H. (2013). Framework for MIMO cross-layer secure communication based on STBC. *Telecommunication Systems*, *52*(4), 2177–2185.
33. Williams, R. T., Prasad, S., Mahalanabis, A. K., & Sibul, L. H. (1988). An improved spatial smoothing technique for bearing estimation in a multipath environment. *IEEE Transactions on Acoustics, Speech and Signal Processing*, *36*(4), 425–432.
34. Xia, T., Zheng, Y., Wan, Q., & Wang, X. (2007). Decoupled estimation of 2-D angles of arrival using two parallel uniform linear arrays. *IEEE Transactions on Antennas and Propagation*, *55*(9), 2627–2632.
35. Xu, X., & Ye, Z. (2012). Two-dimensional direction of arrival estimation by exploiting the symmetric configuration of uniform rectangular array. *IET Radar, Sonar & Navigation*, *6*(5), 307–313.
36. Xu, X., Ye, Z., & Peng, J. (2007). Method of direction-of-arrival estimation for uncorrelated, partially correlated and coherent sources. *IET Microwaves, Antennas & Propagation*, *1*(4), 949–954.
37. Xu, X., Ye, Z., & Zhang, Y. (2009). DOA estimation for mixed signals in the presence of mutual coupling. *IEEE Transactions on Signal Processing*, *57*(9), 3523–3532.
38. Ye, Z., Dai, J., Xu, X., & Wu, X. (2009). DOA estimation for uniform linear array with mutual coupling. *IEEE Transactions on Aerospace and Electronic Systems*, *45*(1), 280–288.
39. Ye, Z., & Liu, C. (2008). On the resiliency of MUSIC direction finding against antenna sensor coupling. *IEEE Transactions on Antennas and Propagation*, *56*(2), 371–380.
40. Ye, Z., & Xu, X. (2007). DOA estimation by exploiting the symmetric configuration of uniform linear array. *IEEE Transactions on Antennas and Propagation*, *55*(12), 3716–3720.
41. Ye, Z., Zhang, Y., & Xu, X. (2009). Two-dimensional direction of arrival estimation in the presence of uncorrelated and coherent signals. *IET Signal Processing*, *3*(5), 416–429.
42. Zhang, Y., Ye, Z., Xu, X., & Cui, J. (2010). Estimation of two-dimensional direction-of-arrival for uncorrelated and coherent signals with low complexity. *IET Radar, Sonar & Navigation*, *4*(4), 507–519.
43. Zhou, Y., & Ng, T. S. (2009). Performance analysis on MIMO-OFCDM systems with multi-code transmission. *IEEE Transactions on Wireless Communications*, *8*(9), 4426–4433.

44. Zhu, H., & Wang, J. (2009). Chunk-based resource allocation in OFDMA systems: Part I: Chunk allocation. *IEEE Transactions on Communications*, *57*(9), 2734–2744.
45. Zhu, H., & Wang, J. (2012). Chunk-based resource allocation in OFDMA systems: Part II: Joint chunk, power and bit allocation. *IEEE Transactions on Communications*, *60*(2), 499–509.

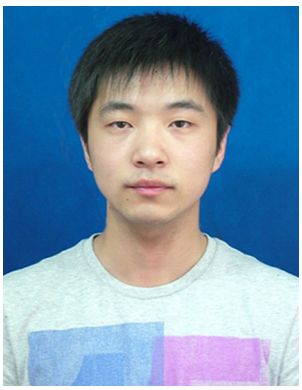

Liangtian Wan received the B.S. degree in Electrical and Information Engineering from Harbin Engineering University, China in 2011. He is currently working toward his M.S. and PhD degree in College of Information and Communication Engineering at Harbin Engineering University. He has served as a reviewer of more than 10 journals. His research interests include array signal processing, compressed sensing and its applications.

Guangjie Han is currently a Professor of Department of Information & Communication System at Hohai University, China. He is also a visiting research scholar of Osaka University from Oct. 2010 to Oct. 2011. He finished the work as a post doctor of Department of Computer Science at Chonnam National University, Korea, in February 2008. He worked in ZTE Company from 2004 to 2006, where he held the position of Product Manager. He received his Ph.D. degree in Department of Computer Science from Northeastern University, Shenyang, China, in 2004. He has published over 120 papers in related international conferences and journals. He has served in the editorial board of up to 14 international journals, including Journal of Internet Technology and KSII Transactions on Internet and Information Systems. He has served as a Co-chair for more than 20 international conferences/workshops; a TPC member of more than 50 conferences. He holds 49 patents. He has served as a reviewer of more than 50 journals. He had been awarded the Best Paper Awards of the ComManTel 2014 and the Chinacom 2014. His current research interests are Sensor Networks, Computer Communications, Mobile Cloud Computing, Multimedia Communication and Security. He is a member of IEEE and ACM.

Joel J. P. C. Rodrigues is a professor in the Department of Informatics of the University of Beira Interior, Covilhã, Portugal, and researcher at the Instituto de Telecomunicações, Portugal. He received a Habilitation from the University of Haute Alsace, France, a PhD degree in informatics engineering, an MSc degree from the University of Beira Interior, and a five-year BSc degree (licentiate) in informatics engineering from the University of Coimbra, Portugal. His main research interests include sensor networks, e-health, e-learning, vehicular delay-tolerant networks, and mobile and ubiquitous computing. He is the leader of NetGNA Research Group (http://netgna.it.ubi.pt), the Chair of the IEEE ComSoc Technical Committee on eHealth, the Past-chair of the IEEE ComSoc Technical Committee on Communications Software, and Member Representative of the IEEE Communications Society on the IEEE Biometrics Council. He is the editor-in-chief of the International Journal on E-Health and Medical Communications, the editor-in-chief of the Recent Advances on Communications and Networking Technology, and editorial board member of several journals. He has been general chair and TPC Chair of many international conferences. He is a member of many international TPCs and participated in several international conferences organization. He has authored or coauthored over 350 papers in refereed international journals and conferences, a book, and 3 patents. He had been awarded the 2014 IEEE ComSoc Multimedia Technical Committee Outstanding Leadership Award, the Outstanding Leadership Award of IEEE GLOBECOM 2010 as CSSMA Symposium Co-Chair and several best papers awards. Prof. Rodrigues is a licensed professional engineer (as senior member), member of the Internet Society, an IARIA fellow, and a senior member of ACM and IEEE.

Weijian Si is currently a Professor of Department of Information & Communication Engineering at Harbin Engineering University, China. He received his Ph.D. degree in College of Information and Communication Engineering from Harbin Engineering University in 2004. He is the person in charge of wide band signals detection, processing and identification in College of Information and Communication Engineering. His research interests include wide band signals detection, high precision passive direction finding and spatial spectrum estimation.

Naixing Feng received the B.S. degree in Electronic Science and Technology and the M.S. degree in Micro- Electronics and Solid-State electronics from Tianjin Polytechnic University, Tianjin, China, in 2010 and 2013, respectively. He is currently working toward his PhD degree in Radio Physics at Xiamen University, Xiamen. His current research interests include computational electromagnetics and acoustics.